Int. j. adv. multidisc. res. stud. 2026; 6(2):1108-1134

Received: 17-02-2026
Accepted: 27-03-2026

International Journal of Advanced Multidisciplinary Research and Studies

ISSN: 2583-049X

Design and Development of a Mini Savonius Wind Turbine for Energy Generation on Flyover Bridges

Hajame Phiri
Department of ICT, Information and Communications University, Zambia, Lusaka, Zambia

DOI: https://doi.org/10.62225/2583049X.2026.6.2.6074
Corresponding Author: **Hajame Phiri**

Abstract
The growing demand for electricity in urban areas has increased the need for alternative and sustainable energy sources. Zambia, at large, heavily depends on hydroelectric power, which faces challenges such as seasonal variability and increasing energy demand. This study explores the feasibility of utilizing mini Savonius wind turbines on flyover bridges within Lusaka as a supplementary energy source. The objective is to harness vehicle-induced wind currents to generate power for urban infrastructure, such as streetlights, traffic signals, and other urban infrastructure, thereby reducing dependence on the national grid.

The Savonius turbine is chosen for its low startup wind speed, omnidirectional operation, and suitability for turbulent urban wind conditions. Additionally, integrating wind energy in urban infrastructure can mitigate vandalism and theft, which are common issues with solar-powered streetlights.

The study highlights the viability of wind energy in urban Zambia and its role in enhancing energy security. Future work will focus on prototype implementation and performance optimization to assess real-world efficiency and economic feasibility.

Keywords: Savonius Wind Turbine, Bridge, Wind Harvesting, Vehicle - Induced Wind, Clean Energy

1. Introduction

The increasing global demand for electricity has driven the exploration of alternative and sustainable energy sources. Renewable energy technologies, such as wind and solar power, have gained widespread attention as viable solutions to reduce dependence on fossil fuels and mitigate environmental degradation. While developed nations have successfully integrated wind energy into their power grids, developing countries, including Zambia, continue to face challenges in diversifying their energy mix.

This proposal focuses on the deployment of a mini Savonius wind turbines on flyover bridges in Lusaka. The objective is to harness wind energy generated by vehicle movement and natural wind currents to supply power for various urban applications, including street lighting, traffic signals, and other public facilities. By introducing these turbines, this study seeks to present a scalable, cost-effective, and sustainable alternative to supplement the electricity supply.

The proposal is crucial as it addresses heavy reliance on hydroelectric power, which accounts for over 80% of the country's total energy supply. Frequent droughts, aging infrastructure like Zesco's distribution poles, and increasing energy demand have led to persistent power shortages and load shedding. Challenges such as theft and vandalism of solar equipment like solar powered streetlights limit its full effectiveness. Incorporating wind energy into the renewable energy mix can enhance energy security and provide a more resilient power solution for urban areas.

This initiative highlights key renewable energy brands and technologies, emphasizing the potential of Savonius wind turbines in urban energy solutions. The main selling point of this proposal is its ability to utilize untapped wind energy from urban traffic flows, creating a unique and practical approach to power generation. By integrating wind power into city infrastructure, this solution showcases an innovative strategy for sustainable urban development.

1.1 Background

Global Perspective on Wind Energy

Wind energy has emerged as one of the fastest-growing renewable energy sources worldwide. Countries such as the United States, China, and Germany have made significant investments in wind power, contributing to a steady increase in global wind energy capacity (International Energy Agency, 2025) [4]. Advances in turbine technology, improved efficiency, and decreasing costs have made wind energy a competitive alternative to fossil fuels. According to the Global Wind Energy Council (GWEC), wind power is expected to contribute significantly to achieving global net-zero targets by 2050 (Global Wind Report, 2025).

Developing nations are also beinning to embrace wind energy as a means to diversify their energy mix, reduce dependence on hydroelectric power, and mitigate climate change impacts. In Africa, countries like South Africa, Egypt, Morocco and Kenya among others, have successfully implemented large-scale wind farms to complement their electricity supply, demonstrating the viability of wind energy in the region (Global Wind Report, 2025). However, challenges such as financing, policy frameworks, and infrastructure limitations have slowed widespread adoption.

Wind Energy in Zambia

Zambia's energy sector is predominantly dependent on hydroelectric power, which contributes over 84% of the country's total electricity generation. However, increasing occurrences of prolonged droughts, exacerbated by climate change, have significantly reduced hydro generation capacity, leading to frequent load shedding that disrupts businesses and households alike (Draft report: Strategic Environmental Assessment of the Energy Sector in Zambia, 2023, p.48). This growing energy insecurity underscores the urgency of diversifying the energy mix through alternative renewable sources, particularly wind power.

Fig 1: BBC. 2024. Hydro-powered Kariba dam [Photo]

Recent assessments by the Ministry of Energy, in collaboration with the World Bank and other stakeholders, reveal that Zambia has viable wind energy potential, particularly in the southern, western, and northeastern regions. Data from the Global Wind Atlas and national wind measurement campaigns indicate annual average wind speeds ranging from 5.9 to 6.4 m/s at 80 meters hub height, with locations such as Lusaka recording average speeds around 6.64 m/s, making them suitable for both small and medium-scale wind energy developments.

Fig 2: Global wind atlas graph results. Source: Global wind atlas [Photo]

Zambia currently has one operational wind power project; the 20 MW Kalumbila Wind Farm in North-Western Province, commissioned in 2020. In addition, 18 wind projects are in the pipeline across eight provinces, with a combined planned capacity of 1,261 MW. The Ministry of Energy has already approved 13 projects, while 5 remain in the planning stages, all spearheaded by private developers (Draft report: Strategic Environmental Assessment of the Energy Sector in Zambia, 2023).

Projections in the Integrated Resource Plan (IRP) estimate that Zambia could achieve wind generation capacities of 1,549 MW by 2026, rising to 2,109 MW by 2030, and 2,884 MW by 2040, positioning wind as a crucial contributor to national energy security, climate resilience, and emissions reduction targets (Draft report: Strategic Environmental Assessment of the Energy Sector in Zambia, 2023).

Despite this potential, wind energy in Zambia remains largely underutilized. Addressing regulatory, technical, and financing barriers, alongside targeted investment in wind measurement infrastructure and grid integration will be vital to unlocking its full potential. Vehicle-Induced Wind from Flyover Bridges.

An innovative approach to wind energy generation in urban settings is the harnessing of vehicle-induced wind. Moving vehicles, especially in high-traffic areas such as flyover bridges, generate considerable wind turbulence. This energy can be captured using Savonius wind turbines, which are well-suited for low wind speeds and urban environments (Wood Mackenzie, 2025) [5]. Deploying mini wind turbines on Lusaka's flyover bridges could provide a decentralized power source for urban applications, reducing strain on the national grid and promoting sustainable energy solutions.

Integrating wind energy from both natural and vehicle-induced sources, can take a significant step toward diversifying Zambia's energy portfolio. This approach not only addresses energy shortages but also contributes to the country's broader renewable energy strategy, ensuring long-term sustainability and resilience.

1.2 Motivation of the Study

The main motivation behind this study is to explore innovative and sustainable energy solutions for Zambia's growing electricity demand. Wind energy, particularly from vehicle-induced wind from flyover bridges. Other than decongestion, flyover bridges can be used to generate wind energy using a mini Savonius wind turbine.

1.3 Significance of the Study

1. Energy diversification: By integrating wind power into Zambia's energy mix, this project reduces reliance on hydroelectricity, mitigating the risks of power shortages.
2. Urban renewable energy solutions: The project introduces an innovative way of harnessing wind energy in city environments, optimizing infrastructure for sustainable development.
3. Public infrastructure efficiency: Mini wind turbines can generate power for streetlights, traffic signals, and other public utilities, reducing energy costs for municipalities.
4. Environmental impact: Utilizing wind energy contributes to the reduction of greenhouse gas emissions and promotes cleaner, greener urban spaces.
5. Economic benefits: Development of this project is cost effective, and will create opportunities for local manufacturing, maintenance, and installation jobs within Zambia's renewable energy sector.

1.4 Scope of the Study

This study focuses on the feasibility and implementation of mini Savonius wind turbines on flyover bridges in Lusaka, to harness vehicle-induced and natural wind currents. The scope includes:

1. Geographical focus: Lusaka's flyover bridges due to their high traffic flow and favorable wind conditions, more than 6.4m/s of the normal wind speed. (Ministry of Energy, 2023) [6] (Global Wind Atlas, 2025) [1].
2. Technology: The study explores the efficiency of Savonius wind turbines, which are suitable for low-speed urban wind conditions.
3. Applications: The generated power will be evaluated for use in street lighting, traffic signals, and other urban facilities, expanding beyond just one application.
4. Energy integration: Assessing the potential contribution of wind energy to reducing dependence on hydroelectricity and complementing other renewable sources like solar.

1.5 Problem Statement

Overdependence on hydropower and solar power has led to inconsistent power supply. As a result, many areas are affected due to loadshedding. Solar streetlights are often vandalized due to the valuable lithium batteries they contain. Therefore, streets remain dark at night, increasing the risk of crime and accidents. This project aims to solve this problem by generation of wind energy using a mini Savonius wind turbine, strategically placing them on flyover bridges. This will help decongest the electrical load from the main grid. Apart from traffic decongestion, flyover bridges can be used to generate this wind energy capitalizing on moving vehicles.

1.6 Objectives

1.6.1 General Objective

The main objective is to design and develop a mini Savonius wind turbine for energy generation on flyover bridges.

1.6.2 Specific Objectives

1. To design a multi-blade Savonius turbine rotor optimized for low-wind-speed operation and high starting torque.
2. To design and construct a power generation and conditioning circuit capable of converting, boosting, regulating, and safely managing the electrical output.
3. To assemble and integrate the turbine rotor, gear system, AC generator, and power generation circuit into a fully functional prototype system.
4. To test the integrated prototype under controlled conditions to validate its performance and operational viability.

1.7 Research Questions

1. What is the optimal design methodology for a multi-blade, mini-scale Savonius rotor to maximize efficiency and power output in low wind speed environments?
2. What is the most effective circuit design for conditioning the variable AC output from the turbine into a stable, regulated 12V DC supply, while incorporating essential protection features like auto cut-off for overvoltage and undervoltage conditions?
3. How can the mechanical components (turbine rotor, gear system) and electrical subsystems (AC generator, power conditioning circuit) be successfully integrated into a single, robust, and functional prototype system?
4. What is the performance of the integrated turbine prototype when tested under controlled wind conditions?

1.8 Definition of Terms

Aspect Ratio: For a Savonius turbine, this is the ratio of the rotor's height to its diameter. A lower aspect ratio generally provides greater structural stability.

Blade Curvature: The degree of bending or shaping of turbine blades.

Buck Converter: A type of DC-DC power converter that steps down voltage while maintaining efficiency.

Charge Controller: An electronic device that regulates the voltage and current from the generator to the battery, preventing overcharging and over-discharging.

Computational Fluid Dynamics (CFD): A simulation tool used to analyse airflow patterns around structures.

Cut-in Wind Speed: The minimum wind speed required to initiate the rotation of a wind turbine and start generating usable power.

Darrieus Wind Turbine: A type of vertical-axis wind turbine that operates on the principle of lift, typically more efficient but with poor self-starting torque compared to the Savonius type.

Energy Storage System (ESS): A system, such as a battery bank, used to store electrical energy.

Flyover Bridge: An elevated road structure designed to cross over other roads or obstacles.

Gear Ratio: The ratio of the number of rotations of the input gear (driven by the turbine) to the output gear (connected to the generator). A higher ratio increases rotational speed.

Low-Wind-Speed Performance: A turbine's ability to start rotating and generate useful power at low wind velocities, a critical characteristic for harvesting vehicle-induced wind.

Overlap Ratio: The horizontal distance between the inner edges of opposing Savonius blades.

Power Coefficient (Cp): A measure of a wind turbine's efficiency in converting kinetic wind energy into mechanical

energy. It is expressed as a ratio of actual power output to the theoretical maximum.

Rectifier: An electrical circuit that converts alternating current (AC) to direct current (DC).

Rotor Solidity: The ratio of the total blade area to the swept area of the rotor. A multi-blade Savonius turbine has high solidity, which contributes to its high starting torque.

Savonius Wind Turbine: A type of vertical-axis wind turbine (VAWT) that operates on the principle of drag. It typically consists of scooped blades and is effective at capturing wind at low speeds, making it suitable for urban environments and turbulent wind conditions.

Starting Torque: The initial force required to set a stationary turbine rotor into motion. Savonius turbines have high starting torque.

Tip-Speed Ratio (TSR): The ratio of the speed of the tip of the turbine blade to the actual wind speed. Savonius turbines have a low TSR.

Torque Coefficient (Ct): A dimensionless parameter that represents the torque produced by a turbine rotor relative to the wind's kinetic energy.

Urban Wind Harvesting: The practice of capturing wind energy from natural or artificial sources within city environments, such as from traffic flow or building-induced wind channels.

Vehicle-Induced Wind: Airflow generated by the movement of vehicles, especially on highways or flyovers.

Vertical-Axis Wind Turbine (VAWT): A wind turbine in which the main rotor shaft is set vertically, allowing it to operate regardless of wind direction.

Voltage Regulator: A device designed to maintain a constant voltage level, protecting the load from voltage fluctuations.

2. Literature Review

2.1 Overview

This chapter reviews existing literature to provide foundational insights into wind energy technologies with a focus on Savonius turbines and urban wind harvesting. The purpose is to highlight their applicability in non-traditional settings such as highways and urban infrastructures where vehicle-induced wind and structural channels like bridges offer untapped energy potential. Reviewing past studies will be done to understand technical viability, efficiency, limitations, and the scope of innovation in integrating wind turbines into dynamic environments like roads and cities.

2.2 Review of Literature

2.2.1 Problem and Research Purpose

The concept of harnessing wind energy for power generation has been around for centuries, with early applications focused on grinding grain and pumping water. However, over the last several decades, the development of wind turbines has evolved significantly, making wind energy one of the fastest-growing renewable energy sources globally. This section presents a review of relevant literature on the various aspects of wind energy, the technologies involved, and the integration of wind turbines into transportation infrastructure, specifically bridges.

The global imperative to transition towards renewable energy sources has catalyzed intense research into efficient energy harvesting technologies (Zemamou, Aggour and Toumi, 2017). Wind energy, as a leading renewable source, is predominantly harnessed by Horizontal Axis Wind Turbines (HAWTs) in large-scale wind farms. However, for small-scale, urban, and low-wind-speed applications, Vertical Axis Wind Turbines (VAWTs) present a more suitable alternative due to their omni-directionality, simplicity, and lower noise emissions (Islam *et al*., 2022). Among VAWTs, the Savonius rotor, operating primarily on drag forces, is particularly advantageous for its superior self-starting capability and performance in turbulent wind conditions (He *et al*., 2019).

The performance of the Savonius Wind Turbine (SWT) has therefore been a subject of extensive research, driven by its potential for distributed energy generation in low-wind-speed and turbulent urban environments. However, the widespread adoption of SWTs is constrained by their characteristically low aerodynamic efficiency, with conventional power coefficient (CpCp) values typically ranging between 0.1 and 0.25 (Zemamou, Aggour and Toumi, 2017). This drawback is primarily attributed to the negative torque generated by the returning blade moving against the wind direction (Mehr and Akhtar, 2024).

The purpose of the present study is to address this efficiency gap by systematically investigating and optimizing a novel design configuration for S-VAWTs. The research will employ computational fluid dynamics (CFD) to explore the synergistic effects of combining optimized blade geometry with advanced flow control devices. Unlike conventional approaches that examine these parameters in isolation, this study will adopt an integrated optimization framework. In addition, it will critically evaluate the methodologies used in prior works, offering a more robust basis for comparing performance improvements.

Source: Socialpyramid, 2023.

Fig 3: Savonius wind turbine [Photo]

2.2.2 Performance Enhancement Strategies

Research efforts to improve SWT performance fall into three broad strands: (1) optimization of intrinsic geometric parameters, (2) implementation of external flow control

devices, and (3) application of advanced computational optimization techniques. Geometric parameter optimization has long been the foundation of SWT research. Studies have investigated parameters such as blade number, aspect ratio (AR), overlap ratio (OR), and twist angle. An experimental study by Wenchenubun *et al*. (2015) compared two-, three-, and four-bladed rotors, revealing a trade-off: the four-bladed design achieved the highest torque, while the three-bladed rotor provided the best tip-speed ratio (TSR) and most stable CpCp performance at higher wind speeds. This suggests that the optimal number of blades depends on whether the design prioritizes starting torque or high rotational speed.

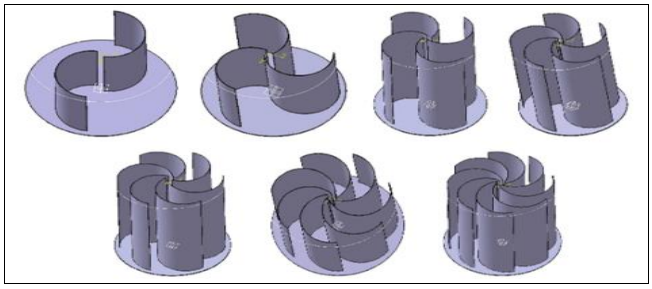

Source: Wenchenubun, 2015.

Fig 4: Savonius multi-blade rotor [Photo]

Similarly, Farozan *et al*. (2025) explored AR, OR, and blade twist, emphasising a practical but often neglected metric: self-starting wind speed. While increasing AR improved peak CpCp, it raised the wind speed required for rotation.

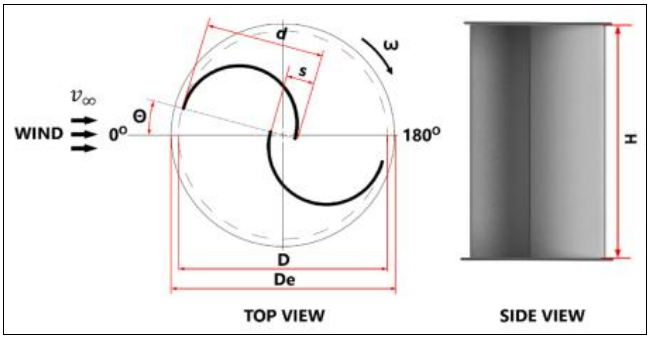

Source: Farozan, 2025.

Fig 5: Top view and side view of Savonius rotor [Photo]

Introducing a 90° blade twist reduced the starting wind speed to 2.5 m/s, significantly enhancing low-speed performance. Their correlation of experimental data with real urban wind conditions revealed that twisted blades could deliver 1.6–5.1 times more average power than conventional designs, despite slightly lower peak CpCp. This finding challenges the conventional emphasis on maximizing CpCp in isolation and underscores the importance of start-up capability for practical deployment.

The synthesis by Chitura *et al*. (2024) reinforces these findings, cataloguing improvements such as a 39% increase in CpCp from scooplet blades and a 30% gain from V-plate deflectors. However, their review highlighted a major deficiency: fewer than 18% of studies examined self-starting behavior, indicating that most research continues to prioritize peak efficiency under steady conditions rather than real-world variability.

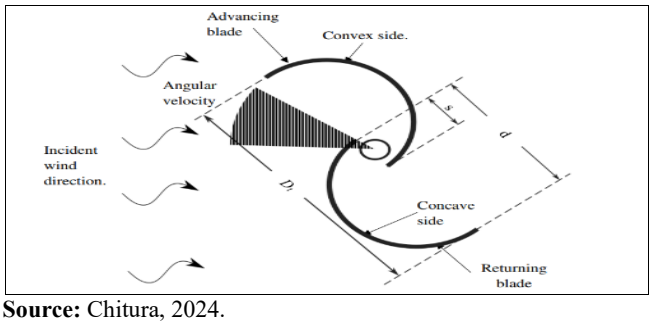

Source: Chitura, 2024.

Fig 6: Detailed Savonius wind turbine rotor blade [Photo]

Moreover, they observed that most studies adjusted one parameter at a time, overlooking multi-parameter interactions that may yield synergistic improvements. Beyond geometry, external flow control devices have been used to mitigate the returning blade's negative torque. Mohamed *et al*. (2010, cited in Zemamou, Aggour and Toumi, 2017) achieved a 27.3% improvement in CpCp by shielding the returning blade with an obstacle, while Mohamed *et al*. (2011) refines this by combining an obstacle with optimized blades, achieving a 38.9% gain. Curtain systems and deflectors have shown further enhancements of up to 38% (Altan and Atilgan, 2008, cited in Zemamou, Aggour and Toumi, 2017). More advanced approaches, such as He *et al*.'s (2019) GA-optimized doubly curved deflector, achieved a remarkable 95.4% improvement. Nevertheless, such devices often compromise omni-directionality, making them less practical for urban or turbulent sites.

The third strand involves computational optimisation and novel blade concepts. He *et al*. (2019) used a genetic algorithm (GA) with CFD to evolve blade geometry, achieving a 33.7% increase in CpCp.

Building on this, Al-Gburi *et al*. (2023) combined CFD with Design of Experiments (DOE) to simultaneously optimize blade number, overlap ratio, and a "guide gap flow" feature. Their factorial approach achieved a 22.8% improvement in CpCp and statistically quantified parameter interactions, with blade number and its interaction with overlap ratio proving most significant. While this represented a methodological leap, they noted limitations: their CFD model excluded the central shaft, leading to overestimated efficiency compared to experiments.

Finally, emerging concepts such as adaptive or deformable blades have introduced further possibilities. Zereg *et al*. (2024) proposed a blade with a deformable trailing edge that dynamically altered pressure distribution during rotation, improving torque by 32% at TSR =1. While promising, such mechanisms introduce mechanical complexity and reliability concerns.

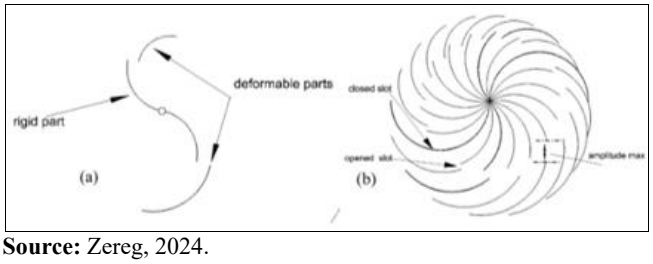

Source: Zereg, 2024.

Fig 7: Deformable Savonius wind turbine rotor [Photo].

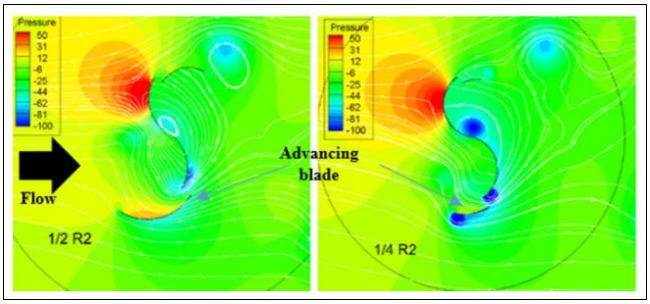

Source: Zereg, 2024.

Fig 8: Comparison of pressure contours [Photo].

2.2.3 Methodological Considerations and Identified Gaps

Despite significant progress, critical methodological shortcomings constrain generalizing of SWT research. Most prominently, many studies rely on two-dimensional CFD simulations, which overpredict turbine performance by neglecting three-dimensional flow effects and tip losses. Mehr and Akhtar (2024) demonstrated that 2D models can significantly exaggerate torque values, whereas their 3D simulations deviated by only ~4% from experimental results. Ferrari *et al*. (2017, cited in Mehr and Akhtar, 2024) similarly warned against uncritical reliance on 2D analyses.

Another limitation is the fragmented approach in existing research. Studies frequently optimise either blade geometry or flow control devices in isolation (Zemamou, Aggour and Toumi, 2017; He *et al*., 2019). Even the advanced DOE framework of Al-Gburi *et al*. (2023) did not incorporate twisted blades, despite their demonstrated impact on start-up performance (Farozan *et al*., 2025). This lack of integration prevents discovery of potential synergies across multiple parameters.

Finally, the drive for higher efficiency often introduces a trade-off between complexity and practicality. Designs involving advanced deflectors or deformable blades frequently undermine the Savonius turbine's key advantages: simplicity, robustness, and omni-directionality (Zereg *et al*., 2024). Yet the literature offers no consistent framework to balance these trade-offs, leaving practitioners with little guidance on how to prioritize efficiency versus simplicity in real-world contexts.

Therefore, the literature exhibits clear gaps. There is a need for high-fidelity 3D CFD-based investigations that integrate optimization of the blade geometries with advanced flow control devices, while explicitly assessing start-up behavior and mechanical complexity. A multi-objective optimization framework addressing these factors could provide a more holistic basis for SWT design, directly bridging the deficiencies identified in prior research.

2.3 Related Works

The concept of harnessing wind energy from moving vehicles is a relatively new area of research, with only a few studies and projects exploring the potential of integrating wind turbines into transportation infrastructure, particularly bridges. This section reviews key studies and related works that have investigated various aspects of wind energy, vehicle-induced wind generation, and the integration of renewable energy technologies into infrastructure. A few are as follows:

2.3.1 Design of an Electrical Power Generating Bridge using Wind Energy from Moving Vehicles by Ngwama, 2025

The core concept involves retrofitting bridges with wind turbines to harness the kinetic energy from wind currents generated by passing vehicles. The technology is based on the aerodynamic principle of vehicle-induced wind. As a vehicle moves at speed, it acts as a blunt body, compressing air in front of it and pushing it to the sides. This action creates a region of low pressure (a vacuum) behind and to the sides of the vehicle. To equalize this pressure, air rushes in from the surroundings, creating significant wind currents and turbulence. This "wake" of moving air possesses kinetic energy. The study proposes to install Vertical Axis Wind Turbines (VAWTs) on the bridge structure to intercept this airflow. The turbines convert the kinetic energy into mechanical rotation, which a generator then converts into electrical energy.

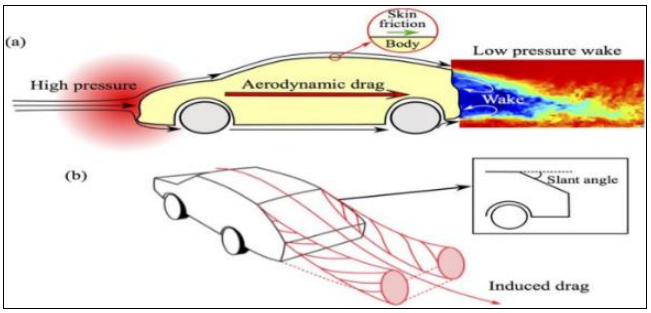

Source: Ngwama, 2025.

Fig 9: Vehicle aerodynamic drag [Photo]

The paper strongly advocates for VAWTs over the more common Horizontal Axis Wind Turbines (HAWTs) for this specific application. The reasons are multi-fold:

Omni-directionality: VAWTs can capture wind from any direction without needing to reorient themselves. This is crucial because the wind from vehicles is highly turbulent and multi-directional.

Structural Integration: Their design allows for the generator and gearbox to be placed at the base, reducing the top-heavy load on the bridge structure and simplifying maintenance.

Performance in Turbulence: VAWTs, particularly the Savonius type, are better suited to operate in the chaotic, low-speed wind conditions typical of vehicle wakes compared to HAWTs, which require steadier, laminar flow for optimal efficiency.

The proposed system is a complete micro-generation and storage setup. The key components, as detailed in the methodology, include:

Energy Capture: VAWTs mounted on the bridge's median and sides.

Power Conversion: A bridge rectifier to convert the Alternating Current (AC) from the turbines to Direct Current (DC).

Voltage Regulation: A voltage stabilizer (like the 7812 IC) to ensure a steady 12V DC output.

Energy Storage: A battery bank charged via a specialized charge controller that prevents overcharging and manages the power input.

Power Distribution: An inverter to convert the stored DC power back to AC (220V) for use by local loads like street lights, traffic signals (robotic circuits), and small buildings.
Safety and Protection: Isolators (fuses or circuit breakers) and Miniature Circuit Breakers (MCBs) are integrated to protect the system from short circuits, overloads, and faults.
The design was validated using Proteus 8.10 Professional simulation software. The simulation modeled the entire power conversion chain, starting with a 120V AC input (simulating the turbine output), stepping it down, rectifying it to a pulsating 12V DC, smoothing it, and finally using it to charge a battery and power an AC lamp via an inverter. The successful simulation demonstrates the technical feasibility of the core electronic system.

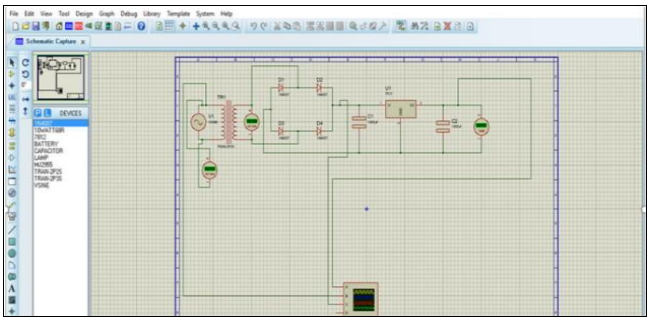

Source: Ngwama, 2025.

Fig 10: Converter circuit diagram [photo]

2.3.2 Experimental Assessment of Suitability of Darrieus and Savonius Turbines for Obtaining Wind Energy from Passing Vehicles by Łyskawiński, Kowalski, and Wojciechowski

This research article presents a meticulous experimental investigation into the most suitable vertical axis wind turbine (VAWT) designs for harvesting wind energy from passing vehicles on highways. The study is grounded in the real-world problem of utilizing a ubiquitous but untapped energy source; the turbulent, multidirectional wind gusts generated by traffic.
The global push for renewable energy, combined with the presence of over 2.5 billion vehicles worldwide, creates a compelling opportunity. The authors identify the "wind waste" produced by these vehicles as a continuous, non-weather-dependent energy source. This energy can be harnessed to power roadside infrastructure like streetlights and signage, potentially creating a self-sustaining system for remote highway sections. The key challenge lies in the nature of this wind: it is highly turbulent, intermittent (dependent on traffic volume), and multidirectional.
A thorough literature review was conducted, noting that while both Horizontal Axis Wind Turbines (HAWTs) and VAWTs have been studied for this application, VAWTs possess inherent advantages. HAWTs require a wind guidance system to always face the wind direction, which is impractical for the chaotic airflow from vehicles. In contrast, VAWTs, specifically Savonius and Darrieus types, can capture wind from any direction, making them ideally suited for this environment. The review also highlighted a reliance on Computational Fluid Dynamics (CFD) simulations in previous studies, which, while valuable, often use simplified 2D models that may not fully capture complex real-world turbulence and 3D effects.

The study's Strength is its Empirical Approach:
Conducted Field Measurements: They first measured actual wind speeds on the S11 expressway in Poland, establishing a realistic operational range of 2.1–8.9 m/s for their experiments, with higher speeds generated by larger vehicles like trucks and buses.

Source: Łyskawiński, Kowalski, and Wojciechowski, 2024.

Fig 11: Vehicle induced wind field test

Selected Turbine Designs: Based on their review, they selected five VAWT designs for testing: two Darrieus (classical and helical) and three Savonius (classical, Bach model, and helical). All turbines were 3D-printed to identical scales (D = H = 140 mm) to ensure a fair comparison.

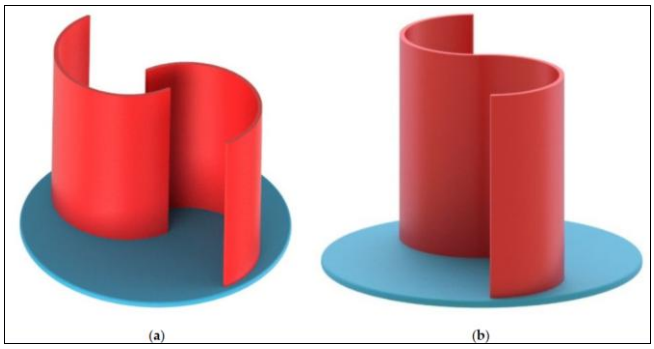

Source: Łyskawiński, Kowalski, and Wojciechowski, 2024.

Fig 12: Savonius turbines: (a) classical; (b) Bach model

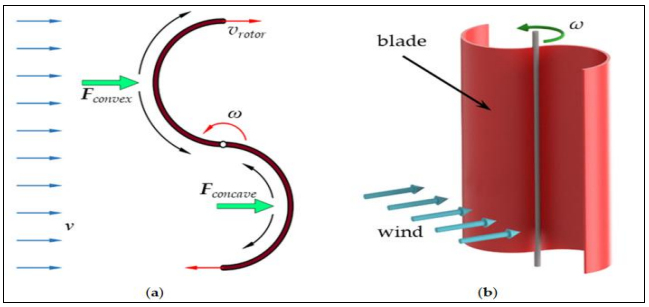

Source: Łyskawiński, Kowalski, and Wojciechowski, 2024.

Fig 13: Savonius turbine aerodynamics: (a) view of cross-section and (b) 3D view

Built a Custom Test Stand: A laboratory wind tunnel with an adjustable-speed fan was used to simulate the wind conditions measured on the highway. This allowed for controlled and repeatable measurements of torque (T) and rotational speed (n) under varying loads.
Derived Key Performance Metrics: From the raw data, they calculated mechanical power (P), tip-speed ratio (λ), and, most importantly, the power coefficient (Cp), which is the measure of a turbine's efficiency in converting wind kinetic energy into mechanical energy.

Detailed experiment found that;
Darrieus turbines confirmed their known weakness: poor self-starting capability. They failed to start at wind speeds below 6 m/s, making them less suitable for the lower-speed gusts from passenger cars. Even when operational, their maximum power output was low (~300 mW).
Savonius Turbines: All three variants demonstrated excellent self-starting at low wind speeds, a critical advantage for intermittent traffic conditions.
Classical & Bach Model: Achieved similar performance, with a maximum power of nearly 800 mW for the Bach model at 8.6 m/s. Their power coefficients (Cp) peaked at around 18%.
Helical Savonius: Emerged as the superior design. It produced more than twice the torque of the other Savonius turbines (nearly 80 Nmm) and achieved the highest efficiency (Cp) of 20.47% at a low wind speed of 5.8 m/s. Its helical design also ensures a smoother, more uniform torque output, reducing vibrations and stress on the system.

Table 1: Rotational speed versus wind speed for turbines: Bach model, classic Savonius and helical Savonius

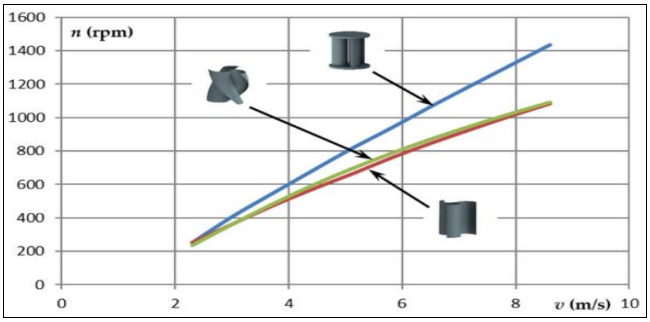

Source: Łyskawiński, Kowalski, and Wojciechowski, 2024

2.3.3 Renewable Energy Generation from Vehicles Motion Using Wind Turbine-Based MATLAB Simulation by Abdullah Alsahli, Mansour Alajmi, Saud Almutairi and Saleh Buolayyan

The fundamental principle for this research is that the kinetic energy of wind, proportional to the cube of its velocity, can be captured. On highways, this wind is not ambient but is "induced" by the movement of vehicles. As vehicles displace air, they create a wake of turbulent, high-velocity airflow. This represents a significant, untapped energy source. The expansion here involves understanding the aerodynamic profile of different vehicles. A sedan, for example, will create a different wake pattern and wind speed compared to a large truck or lorry. As highlighted, Computational Fluid Dynamics (CFD) analyses, such as those using ANSYS Fluent, are crucial for modeling these complex interactions. These simulations help visualize the velocity vectors and pressure differentials around vehicles, allowing researchers to identify optimal placement for turbines, whether at the roadside, on medians, or directly on lighting poles; to intercept the most energetic parts of the wake.

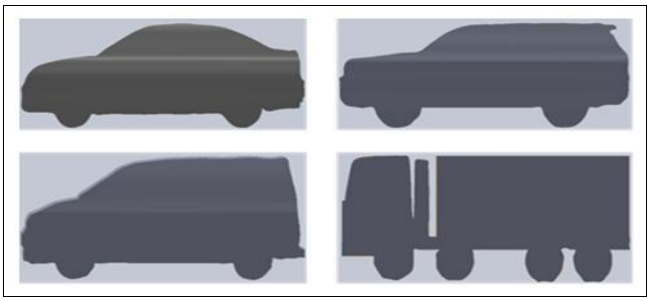

Fig 14: Abdullah Alsahli, Mansour Alajmi, Saud Almutairi and Saleh Buolayyan. The four 3D vehicle types

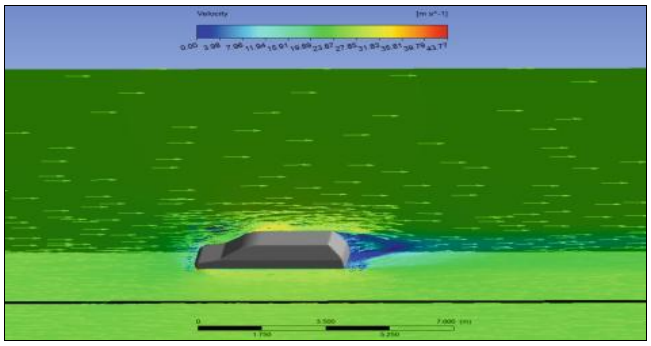

Fig 15: Abdullah Alsahli, Mansour Alajmi, Saud Almutairi and Saleh Buolayyan. Typical velocity vectors resulted from vehicle movement

The choice of a Vertical-Axis Wind Turbine (VAWT) over a Horizontal-Axis Wind Turbine (HAWT) is well-justified and is a consensus in this field. The key reasons are:
Omni-directionality: VAWTs do not need to yaw into the wind, making them perfectly suited for the chaotic, multi-directional gusts produced by passing vehicles.
Lower Noise: This is critical near residential areas adjacent to highways.
Easier Maintenance: With the generator and gearbox often located at ground level, maintenance is simpler and safer.
The expansion delves into the trade-offs between different VAWT types:
Savonius Turbines (Drag-based): Excellent at self-starting and performing in low, turbulent winds, but have a lower tip-speed ratio and efficiency.
Darrieus Turbines (Lift-based): More efficient than Savonius turbines but poor at self-starting and can suffer from structural fatigue.
Hybrid Designs (e.g., Helical Savonius): These aim to combine the self-starting capability of Savonius with the higher efficiency of Darrieus designs, representing a current trend in optimization.

2.3.4 Investigation of an Innovative Savonius Turbine in Practice by R. Afify, E. Saber & H. Awad

This study addresses a fundamental limitation of the Savonius wind turbine: its inherent low efficiency due to negative torque. Negative torque is generated when the convex side of the blade rotates into the wind, creating significant drag that opposes the turbine's motion.

The core innovation for this research is the flapping gates system integrating lightweight "flapping gates" into the blades of the Savonius turbine.

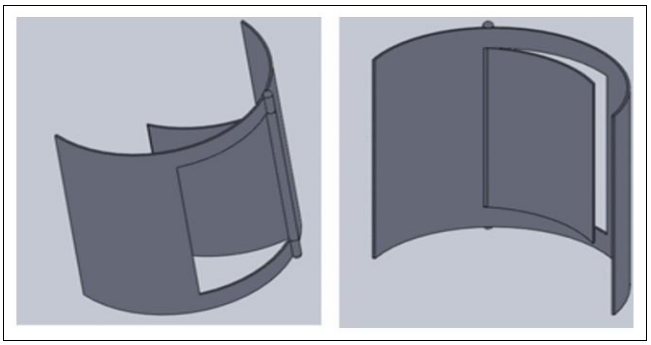

Fig. 16: R. Afify, E. Saber & H. Awad. 2025 [14]. Savonius rotor blade with flapping gates

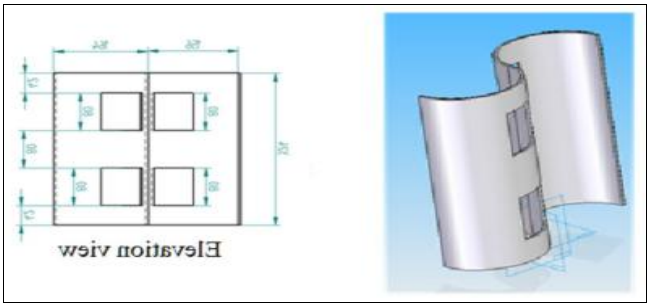

Fig 17: R. Afify, E. Saber & H. Awad. 2025 [14]. Savonius rotor blade with flapping gates elevated view

These gates are small, hinged panels distributed across the blade's surface. Their operation is passive and intelligent, governed by the interplay of two physical forces:

Aerodynamic pressure force (p): This force, exerted by the wind, acts to push the gate open. Centrifugal Force (Fc): This force, resulting from the rotation of the turbine, acts to pull the gate closed.

The behavior of these gates differs depending on which side of the blade is facing the wind:

On the concave (advancing) blade: This blade generates positive torque. Here, both the pressure force and the centrifugal force act in the same direction, keeping the flapping gates firmly closed. This preserves the high-drag, torque-producing profile of the concave surface.

On the Convex (Returning) Blade: This blade typically generates negative torque. The novel mechanism comes into play here: The pressure force acts to open the gate. The centrifugal force acts to close it.

The gate's position is thus dynamically controlled. At lower rotational speeds, the pressure force dominates, opening the gate and allowing air to flow through the blade. This "venting" effect drastically reduces the drag force on the convex blade, thereby reducing the negative torque. Furthermore, the design of the gate creates a nozzle effect, accelerating the exiting air and generating a thrust force (F_th). This thrust acts in the direction of the turbine's rotation, actively contributing positive torque instead of just reducing negative torque.

The research employed a rigorous two-stage experimental setup to validate the concept.

First set of experiments (proof of concept): A small-scale turbine was placed inside a wind tunnel. A single flapping gate was installed on each blade. The results were clear: the modified turbine produced 16.23% more power on average at wind speeds between 6.3 and 11.5 m/s. At very high speeds, the centrifugal force closed the gates, causing the modified turbine to perform identically to the conventional one, confirming the physical model.

Second set of experiments (performance quantification): A larger, more instrumented turbine was tested outside the wind tunnel exit. This setup allowed for detailed measurements of static torque, torque coefficient, and power coefficient.

Static Torque: The modified rotor demonstrated significantly higher static torque and static torque coefficient across all angular positions, proving its superior self-starting capability and inherent torque advantage.

Power and Torque Coefficients: The modified design consistently outperformed the conventional one.

The torque coefficient (Ct) was up to 23.83% higher at low tip speed ratios (TSR). The power coefficient (Cp) showed an average increase of 25% at medium TSRs and a 16.91% improvement at higher TSRs.

2.4 Gaps in Literature

Recent advancements in renewable energy have explored the potential of Savonius wind turbines for harnessing vehicle-induced wind on highways and bridges (Ngwama, 2025; Afify, Saber, & Awad, 2025 [14]). However, the existing body of research predominantly focuses on large-scale energy generation and grid integration, overlooking targeted, small-scale applications for direct urban infrastructure support. An application gap exists in the design and development of miniaturized Savonius turbine systems specifically intended to power streetlights on flyover bridges. This gap is critical, as it represents a direct, sustainable solution to public lighting needs that is less susceptible to vandalism compared to solar-based systems.

Furthermore, the literature reveals a pronounced geographical and economic bias. Studies are primarily contextualized within high-income countries and lack comprehensive techno-economic analyses that scrutinize the operational costs, maintenance logistics, and total lifespan, which is important for assessing viability in developing nations. This is compounded by an environmental integration gap, where key factors like seasonal rain patterns, ambient temperature, and specific road geometry are seldom integrated into performance models, leading to inaccurate predictions.

From a design perspective, research has primarily aimed to minimize the negative drag on the convex blade, treating it as a liability rather than exploring innovative mechanisms to harness it as a potential asset. Concurrently, a structural and manufacturing gap is evident in the overwhelming focus on optimizing single, monolithic blade structures, overlooking the potential benefits of modular or segmented designs for production and maintenance.

There is a clear need for research that moves beyond theoretical energy potential and focuses on the practical, context-sensitive development of a deployable, mini Savonius wind turbine system to reliably power flyover streetlights in developing nations like Zambia, thereby enhancing urban safety and energy independence.

3. Methodology

3.1 Overview

This chapter outlines the research methodology adopted for

the design and development of a mini Savonius wind turbine for energy generation on flyover bridges, with a specific focus on vehicle-induced wind. The methodology details the research approach, the design framework, the data collection methods, and the tools and techniques used to explore the feasibility and effectiveness of integrating wind turbines into transportation infrastructure.

The study employs a primarily practical approach, combining theoretical insights from recent research with physical data collection from real-world traffic conditions. This dual strategy ensures that the research conclusions are both theoretically sound and practically applicable.

This chapter also provides a justification for the selected research tools and techniques. These include a simple electrical circuit design, a multi-blade mini Savonius wind turbine model, and a simple gear system. The data collected through these methods will directly inform the design and operational requirements for wind turbines suitable for installation on flyover bridges. Through this methodology, the study aims to contribute valuable insights into integrating renewable energy systems in urban settings, with potential for future implementation in Zambia and other regions experiencing power shortages.

3.2 Research Design

This study will adopt an experimental and practical development research design. This methodology is selected because the primary objective is to create a functional mini Savonius wind turbine system and to evaluate its performance. The research design involves a cyclical process of designing, constructing, testing, and refining a physical prototype based on both theoretical principles and data collected from real-world conditions. This approach ensures the findings are grounded in practical application and directly address the problem of energy generation for streetlights on flyover bridges.

3.3 Baseline Study

The baseline study establishes the foundational performance targets and real-world operating conditions that the turbine system must be designed to meet. This phase involves characterizing the specific environment of a selected flyover bridge by collecting quantitative data on key parameters, including traffic density, average vehicle size, and ambient wind patterns. Additionally, it defines the minimum energy output required to power a standard 12V DC LED streetlight for this study. This baseline provides the critical reference points against which all subsequent design decisions and prototype performance will be measured and validated.

3.3.1 Data Collection

The data collection process will involve a preliminary assessment of the wind energy potential using a residential house rooftop and a selected flyover bridge to determine baseline viability. A digital multimeter will be used to measure voltage and current output. By correlating these electrical readings with observed wind conditions, an estimate of the available wind power will be established to inform the initial design requirements for the Savonius turbine prototype.

3.3.2 Research Approach

The research will follow an experimental, iterative approach centered on prototyping and experimental testing. The process will begin by constructing a physical prototype based on established principles. This prototype will then undergo testing to measure its initial performance. The development phase will include designing a converter circuit to rectify, boost, and regulate the turbine's output to a stable DC voltage, and connecting a gear system to increase the rotational speed input to the generator. An LED light will serve as the system load for testing. This cycle of testing the assembled system under different conditions and making design refinements will continue until the prototype meets the performance targets established in the baseline study, ensuring a functional and optimized final design.

3.3.3 System Design

This study will employ an experimental method to develop and validate the energy system. The system will be designed around a multi-blade Savonius wind turbine constructed from PVC material. A simple 3:1 gear system will be implemented to increase the rotational speed from the turbine to the AC generator, which will act as the system's voltage source. The electrical subsystem will consist of a bridge rectifier to convert AC to DC, a transformer to step up the voltage, a voltage regulator for protection against under-voltage or over-voltage conditions, and a relay for additional load protection. The complete system will be validated using an LED light as the final load.

3.4 System Design

3.4.1 Block Diagram

1. Savonius Wind Turbine Block Diagram

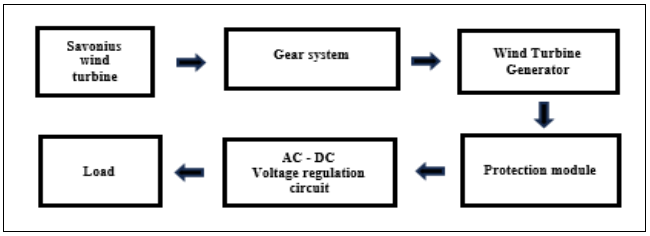

Fig 18: Savonius wind turbine block diagram

Savonius Wind Turbine

A vertical-axis wind turbine that is designed to harness wind energy and convert it into mechanical rotational motion.

Gear System

A mechanical interface that increases the rational speed from the turbine shaft to compensate the low RPM of Savonius wind turbine.

AC Generator

Converts mechanical rotation into alternating current (AC), supporting bidirectional rotation.

Protection Module

The protection module serves to secure the linked electrical hardware. Its fundamental purpose is to regulate the produced electrical output from the generator, thereby mitigating risks associated with excessive voltage and current.

Voltage Regulation Circuit

This includes a bridge rectifier to convert AC to DC, followed by filter capacitors and voltage regulator to ensure smooth and constant DC output.

Load
Device or system powered by the wind turbine, such as lighting.

3.4.2 Detailed System Design

1. System Design: Savonius Wind Turbine

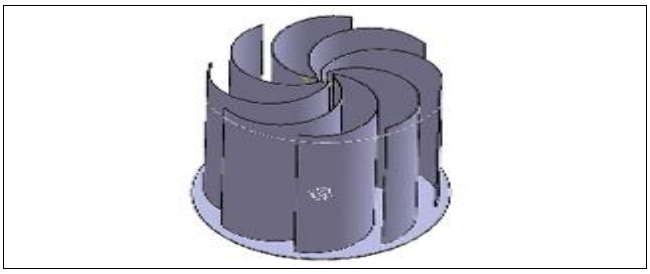

Fig 19: Example of a multi-blade Savonius wind turbine rotor

The core of the system is a multi-blade Savonius rotor. A primary reason for selecting a multi-blade configuration is to achieve a low overlap ratio, which refers to the spacing between the inner edges of opposing blades. A lower overlap ratio is beneficial as it minimizes wind leakage between the blades, thereby increasing the pressure differential across the rotor and significantly enhancing the starting torque. This is crucial for ensuring the turbine can self-start effectively in the low and gusty wind conditions typical on a flyover. Furthermore, it improves structural stability, reduces bending stress on the blades, and makes the turbine more compact and suitable for installation on infrastructure.

The blades will be constructed from Polyvinyl Chloride (PVC) material. PVC is selected for its lightweight properties and ease of fabrication. The low weight of PVC reduces the rotor's startup torque, enabling it to begin rotating at very low wind speeds. While less rigid than metals like aluminium, PVC offers sufficient durability for this application and allows for low-cost, rapid prototyping and modification using simple tools. Additional advantages include its high resistance to corrosion, which is essential for an outdoor environment, its low cost and wide availability, and its smooth surface finish, which helps maintain aerodynamic efficiency. This combination of properties makes PVC an ideal material for developing a functional, cost-effective, and responsive turbine prototype.

Wind Energy Formular

According to Johnson, Pao, Balas, and Finger (2006) [15], the power coefficient Cp is defined as the ratio of the aerodynamic rotor power P to the power (Pwind) available from the wind. where ρ is the air density, A is the rotor swept area, and v is the wind speed. The aerodynamic rotor power is given by:

$$C_p = \frac{P}{P_{\text{wind}}}.$$

The available power P_{wind} is given by

$$P_{\text{wind}} = \tfrac{1}{2}\rho A v^3,$$

The aerodynamic rotor power is given by:

$$P = \tau_{aero}\omega$$

Where;

τaero is the aerodynamic torque applied to the rotor by the wind and **ω** is the rotor angular speed given by:

$$\omega = \frac{2\pi N}{60}$$

Where;
N is the rotational speed (RPM)
2π is the number of radians in one full revolution.
60 is the number of seconds in a minute.

Wind mills convert Kinetic Energy (KE) of the wind into Mechanical Energy. The total power of the wind stream is equal to the time rate of kinetic energy. The wind mill with large swept area produces more power. Wind velocities below 5 m/s and above 25 m/s are not suitable for wind turbines.

$$\text{Kinetic Energy} = \quad K\ E = \tfrac{1}{2}mv^2$$

$$\text{Mass flow rate} = \rho \times A \times \text{Velocity}$$

Where: ρ is density

$$\text{K.E per Unit Volume} = \frac{1}{2}\rho A \times V^2$$

The Total Power (Pt) in the wind is:
Kinetic energy multiplied by Velocity, that is;

$$P_t = \frac{1}{2}\rho \times \frac{\pi D^2}{4} \times V^3 = \frac{1}{8}\rho \times \pi D^2 \times V^3$$

This assembly begins with the physical turbine, the blades constructed from a 75mm diameter PVC pipe that is precisely cut in half to create the characteristic scooped aerodynamic profile. These halves are meticulously joined using nails and glue to form a robust, multi-blade mini Savonius rotor.

For the experimental setup, the rotor blades were fabricated by cutting two different sizes of PVC water pipes. The larger pipe was bisected longitudinally to create the primary curved turbine blades.

These blades were securely affixed to a smaller diameter PVC pipe, which acts as a central shaft or hub. This connection was reinforced with both adhesive and mechanical fasteners (nails) to ensure a rigid assembly. This central shaft was then mounted onto a metal shaft via bearings, which provide a low-friction pivot point for smooth rotation.

The metal shaft is coupled to a gear train salvaged from a disused standing fan. This gear system subsequently drives the motor, which acts as a generator.

Fig 20: 75mm diameter pipe

Fig 21: Mini Savonius wind turbine rotor

The rotor is mechanically coupled to a bearing that acts as a low-friction pivot, enabling smooth rotation. This entire rotating assembly is securely mounted on a metal stand, which also houses the integrated gear system for rotational speed amplification and the AC generator that converts the mechanical energy into electrical output. By using a laboratory AC source to emulate the electrical output of this mechanical system, the research achieves a critical decoupling of variables. This methodology allows for the precise and safe testing, calibration, and validation of the entire power conditioning circuit; including the rectifier, voltage regulator, and auto cut-off protection under controlled and repeatable conditions. This step is fundamental to achieving the project's goal, as it ensures that the custom-designed electronics are fully optimized and proven reliable before facing the unpredictable and variable forces of real-world vehicle-induced wind on a flyover bridge, thereby de-risking the final integration and deployment phase.

Fig 22: Bearing rings for pivot

The vast majority of vehicles on Munali Flyover Bridge are the lightweight vehicles including cars and trucks move at speed of (60-100 km/h). What actually stands out is the significant dissipation in the magnitude and fluctuations of localized wind which increases from the passing trucks than small cars. Therefore, the ideal position of a harvesting energy device should be as close as possible to the moving vehicle positioning on the median and sides of the motorway will ensure a safe and constant distant regardless of vehicle type. Since there is no experimental data in regard to the performance of Savonius vertical axis wind turbine (VAWT) on highways and there are tons of vehicles passing through highways and motorways with appreciable speeds. Each of these moving vehicles is an energy source. Theoretically, a portion of this energy can be harvested by laying a drag based vertical axis wind turbine (VAWT) in the vicinity of passing vehicles. Some studies show that in addition to the kinetic component of this wind, the vortices shed by each moving vehicle can induce the flow field as the figure below. These swirling flow structures can assist the rotor for more torque generation if its blades benefit from an appropriate design. The generated electricity can be utilized in many worthwhile applications.

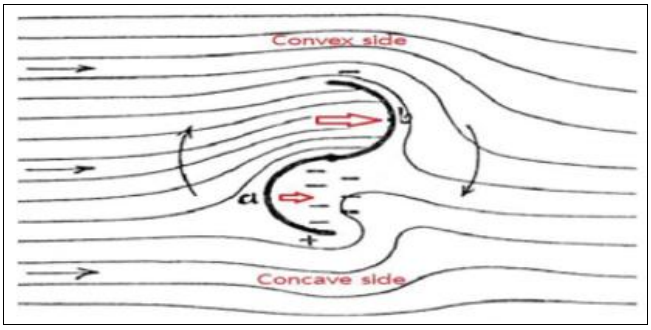

Fig 23: Direction of rotation due to drag

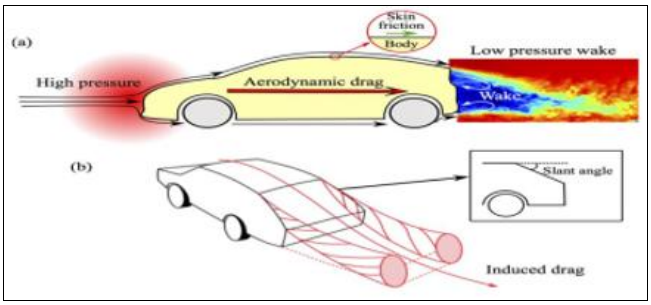

Source: Ngwama 2025

Fig 24: How wind drag is created

Source: Spannovation Group

Fig 25: Munali flyover bridge

Source: Lusaka Times Media

Fig 26: Munali flyover bridge close-up

2. System Design: Gear System

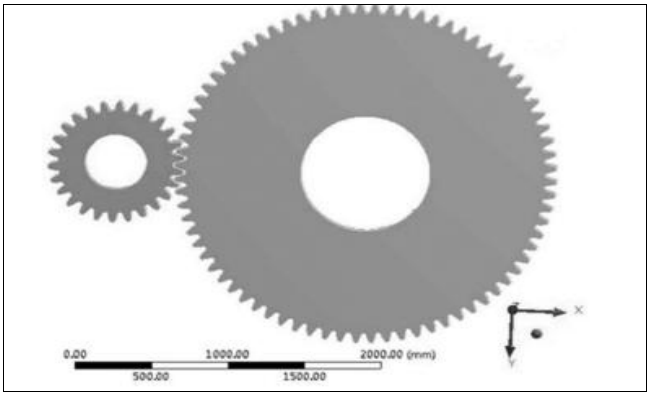

Fig 27: Gear system

A gear ratio of 3:1 will be implemented in the system to increase the rotational speed delivered from the turbine shaft to the AC generator. This speed multiplication is essential for enabling the generator to produce a higher frequency and more usable voltage level even when the turbine is rotating at low speeds caused by light vehicle winds. Beyond increasing rotational speed, this fixed gear ratio provides a mechanical advantage that improves the system's torque transmission efficiency and ensures more consistent power generation from the highly variable input winds. The chosen ratio offers an optimal balance, providing significant speed increase without introducing excessive mechanical complexity or friction losses that could hinder performance at very low starting torques.

3. Wind Turbine Generator

One of limiting factors in wind turbines lies in their generator technology. Traditionally, there are three main types of wind turbine generators (WTGs) which can be considered for the various winds turbine systems, these being:

- Direct current (DC).
- Alternating current (AC) synchronous generators.

In principle, each can be run at fixed or variable speed. Due to the fluctuating nature of wind power, it is advantageous to operate the WTG at variable speed which reduces the physical stress on the turbine blades and drive train, and which improves system aerodynamic efficiency and torque transient behaviours.

(a) DC Generator Technologies

In conventional DC machines, the field is on the stator and the armature is on the rotor. The stator comprises a number of poles which are excited either by permanent magnets or by DC field windings. If the machine is electrically excited, it tends to follow the shunt wound DC An example of the DC wind generator system is illustrated in the figure below. For shunt wound DC generators, the field current (and thus magnetic field) increases with operational speed whilst the actual speed of the wind turbine is determined by the balance between the wind turbine drive torque and the load torque. The rotor includes conductors wound on an armature which are connected to a split-slip ring commentator. Electrical power is extracted through brushes connecting the commentator which is used to rectify the generated AC power into DC output. Clearly, they require regular maintenance and are relatively costly due to the use of commutators and brushes.

In general, these DC wind turbine generators are unusual in wind turbine applications except in low power demand situations where the load is physically close to the wind turbine, in heating applications or in battery charging. generator concept.

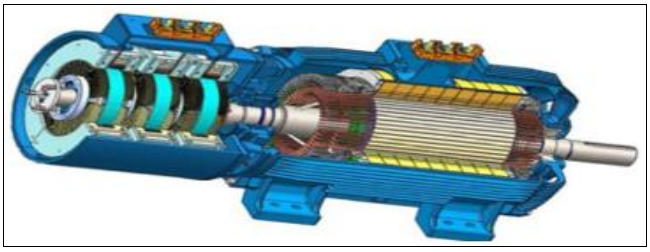

Fig 28: Cutaway of a doubly-fed induction generator with a rotary transformer

(b) AC Synchronous Generators

Since the early time of developing wind turbines, considerable efforts have been made to utilize three-phase synchronous machines. AC synchronous WTGs can take constant or DC excitations from either permanent magnets or electromagnets and are thus termed PM synchronous generators (PMSGs) and electrically excited synchronous generators (EESGs), respectively. When the rotor is driven by the wind turbine, a three-phase power is generated in the stator windings which are connected to the grid through transformers and power converters. For fixed speed synchronous generators, the rotor speed must be kept at exactly the synchronous speed.

Synchronous generators are a proven machine technology since their performance for power generation has been studied and widely accepted for a long time. A cutaway diagram of a conventional synchronous generator is shown. In theory, the reactive power characteristics of synchronous WTGs can be easily controlled via the field circuit for electrical excitation. Nevertheless, when using fixed speed synchronous generators, random wind speed fluctuations and periodic disturbances caused by tower-shading effects and natural resonances of components would be passed onto the power grid. Furthermore, synchronous WTGs tend to have low damping effect so that they do not allow drive train transients to be absorbed electrically. As a consequence, they require an additional damping element (e.g. flexible coupling in the drive train), or the gearbox assembly mounted on springs and dampers. When they are integrated into the power grid, synchronizing their frequency to that of the grid calls for a delicate operation. In addition, they are generally more complex, costly and more prone to failure than induction generators. In the case of using electromagnets in synchronous machines, voltage

control takes place in the synchronous machine while in permanent magnet excited machines, voltage control is achieved in the converter circuit.

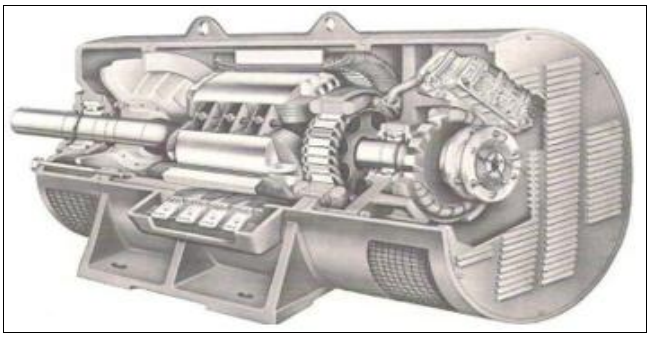

Fig 29: Cutaway of a doubly-fed induction generator with a rotary transformer

In recent decades, PM generators have been gradually used in wind turbine applications due to their high-power density and low mass. Often these machines are referred to as the permanent magnet synchronous generators (PMSGs) and are considered as the machine of choice in small wind turbine generators. The structure of the generator is relatively straightforward. As shown in the rugged PMs are installed on the rotor to produce a constant magnetic field and the generated electricity is taken from the armature (stator) via the use of the commutator, slip rings or brushes. Sometimes the PMs can be integrated into a cylindrical cast aluminium rotor to reduce costs. The principle of operation of PM generators is similar to that of synchronous generators except that PM generators can be operated asynchronously. The advantages of PMSGs include the elimination of commutator, slip rings and brushes so that the machines are rugged, reliable and simple. The use of PMs removes the field winding (and its associated power losses) but makes the field control impossible and the cost of PMs can be prohibitively high for large machines.

Because the actual wind speeds are variable, the PMSGs cannot generate electrical power with fixed frequency. As a result, they should be connected to the power grid through AC-DC-AC conversion by power converters. That is, the generated AC power (with variable frequency and magnitude) is first rectified into fixed DC and then converted back into AC power (with fixed frequency and magnitude). It is also very attractive to use these permanent magnet machines for direct drive application. Obviously, in this case, they can eliminate troublesome gearboxes which cause the majority of wind turbine failures. The machines should have large pole numbers and are physically large than a similarly rated geared machine.

Working Principle of a Synchronous Generator

A synchronous motor is an AC motor because its rotational speed is constant equal to that of a synchronous speed machine. Synchronous motors are mainly used as generators, but also as motors and regulators. Synchronous generators are designed according to the principle of electromagnetic induction, which converts mechanical energy into electrical energy through the relative motion between the rotor magnetic field and the stator windings. After the rotor coil enters the direct current, a magnetic field is generated. When the rotor rotates at n speed under the driving of external force, the magnetic field of the rotor and the stator conductor have relative motion, that is, the stator conductor cuts the magnetic wire, and an induced potential is generated. When the rotor rotates continuously at a constant speed, the alternating current potential cycle on the stator coils is constantly changing, which is the working principle of a synchronous generator.

The overhaul period of synchronous generators for diesel generator sets is generally 2-4 years. The main contents of the overhaul include disassembling the body, disassembling the rotor, repairing the stator, repairing the rotor, checking the state of the slip ring, installing the generator and insulating the axis.

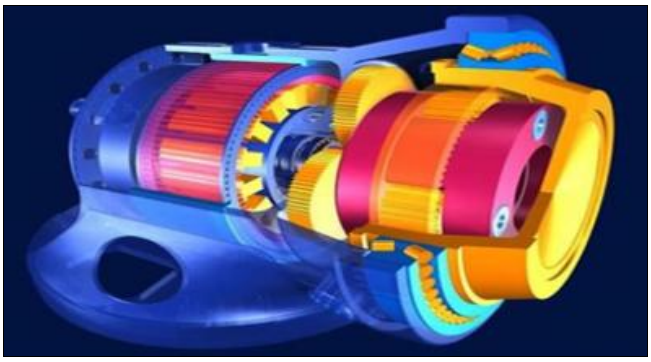

Fig 30: Cross-section cutaway of a permanent magnet synchronous generator

A potential variant of synchronous generators is the high temperature superconducting generator for a multi-MW, low-speed HTS synchronous generator system. The machine comprises the stator back iron, stator copper winding, HTS field coils, rotor core, rotor support structure, rotor cooling system, cryostat and external refrigerator, electromagnetic shield and damper, bearing, shaft and housing. In the machine design, the arrangements of the stator, rotor, cooling and gearbox may pose particular challenges in order to keep HTS coils in the low temperature operational conditions.

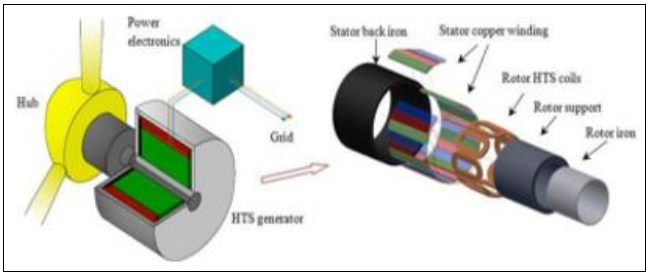

Fig 31: generator Schematic of a HTS synchronous generator system

4. Protection Module

Miniature Circuit Breaker Construction (MCB)

The miniature circuit breaker (MCB) plays an important role in providing overcurrent protection and a disconnect means in electrical networks. A breaker is a device designed to isolate a circuit during an overcurrent event without the use of a fusible element. A breaker is a resettable protective device that protects against two types of overcurrent situations:

1. Overload
2. Short Circuit

MCB Construction

(a) Thermal / Magnetic Trip Units

Current Limiting Breakers use an electromechanical (Thermal /Magnetic) trip unit to open the breaker contacts during a overcurrent event. The thermal trip unit is temperature sensitive and the magnetic trip unit is current sensitive. Both units act independently and mechanically with the breaker's trip mechanism to open the breaker's contacts.

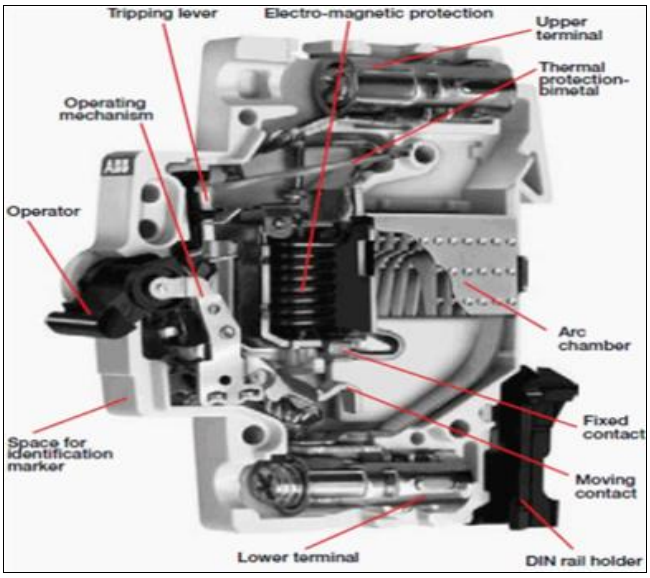

Fig 32: Miniature circuit breaker

In the case of short circuit conditions, the current rises suddenly in an unpredictable way, leading to the electromechanical displacement of the plunger associated with a solenoid. The plunger hits the trip lever, which causes the automatic release of the latch mechanism by opening the circuit breaker contacts.

An MCB is a simple, easily operable device and is maintenance-free too. MCB can be easily replaced. The trip unit is the key part of the MCB – Miniature Circuit Breaker on which the unit operates. The bi-metal present in the MCB circuit protects against overload current, and the electromagnet in the circuit protects against short-circuit current.

(b) Overload Protection

The thermal trip unit protects against a continuous overload. The thermal unit is comprised of a bimetal element located behind the circuit breaker trip bar and is part of the breaker's current carrying path. When there is an overload, the increased current flow heats the bimetal causing it to bend. As the bimetal bends it pulls the trip bar which opens the breaker's contacts. The time required for the bimetal bending and trip the breaker varies inversely with the current. Because of this, the tripping time becomes quicker as current increases in magnitude. Overload protection is applicable to any installation, conductor, or component which can be subjected to low-magnitude but long-time over-currents. Low-magnitude, long-time over-currents can be dangerous because they reduce the life of the electrical installation, conductor, and components and if left unchecked could result in fire.

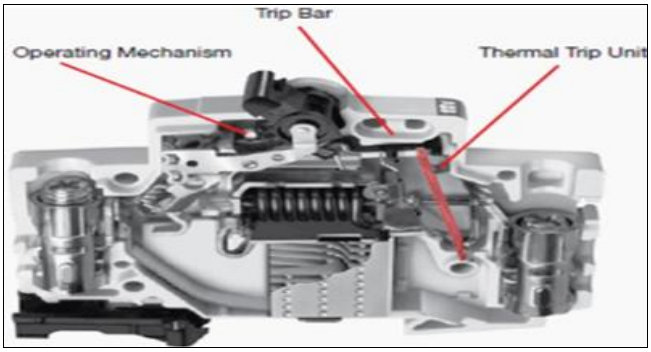

Fig 33: An overload protection unit breaker

(c) Magnetic Trip Units (Short Circuit Protection)

The Magnetic trip unit protects against a short circuit. The magnetic trip unit is comprised of an electromagnet and an armature.

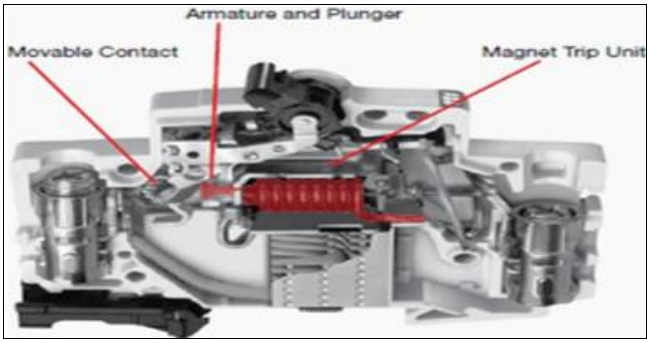

Fig 34: A magnetic strip

Working Principle of a Magnetic Strip

When there is a short circuit, a high magnitude of current passes through the coils creating a magnetic field that attracts the movable armature towards the fixed armature. The hammer trip is pushed against the movable contact and the contacts are opened. The opening of the breakers contacts during a short circuit is complete in 0.5 milliseconds.

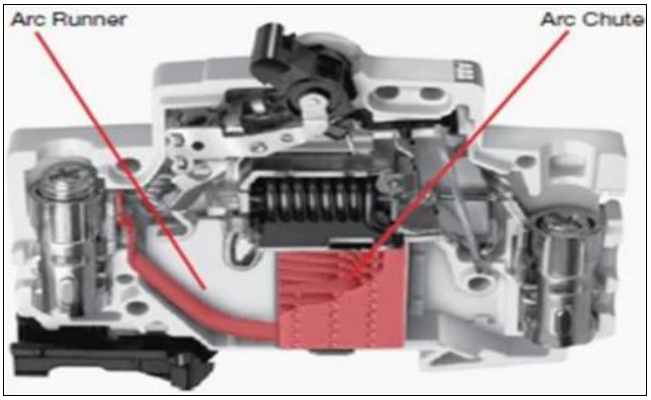

Fig 35: Magnetic strip components

(d) Arc Runners / Arc Chutes

The arc runner and arc chute limit and dissipate the arc energy during the interruption of an overload or short circuit event. During an overload or short circuit event, the contacts of the breaker separate and an electrical arc is formed between the contacts through air. The arc is moved into the

arch chute by "running" the arc down the interior of the breaker along the arc runner. When the arc reaches the arc chute it is broken into small segmented arcs. The segmented arcs split the overall energy level into segments less than 25V. Each 25V segment does not have a high enough energy level to maintain an arc and all energy is naturally dissipated.

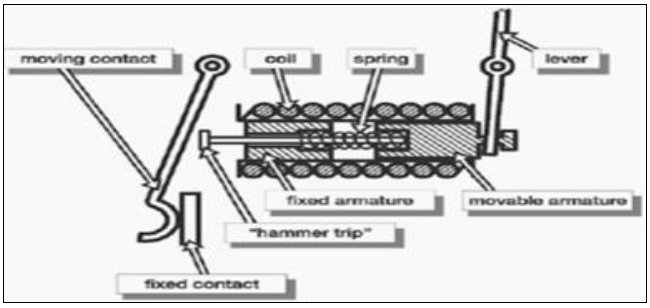

Fig 36: Arc runner / arc chute

Thermal Trip Unit

The first sloping region of the breaker curve is a graphical representation of the tripping characteristics of the thermal trip unit. This portion of the curve is sloped due to the nature of the thermal trip unit. The trip unit bends to trip the breaker's trip bar in conjunction with a rise in amperage (temperature) over time. As the current on the circuit increases, the temperature rises, the faster the thermal element will trip.

Magnetic trip unit region of the breaker curve is the instantaneous trip unit. MCB – miniature circuit breaker's instantaneous trip unit interrupts a short circuit in 2.3 to 2.5 milliseconds. Because of this, the curve has no slope and is graphically represented as a vertical straight line.

5. 12V Converter Circuit with Auto Cut-off

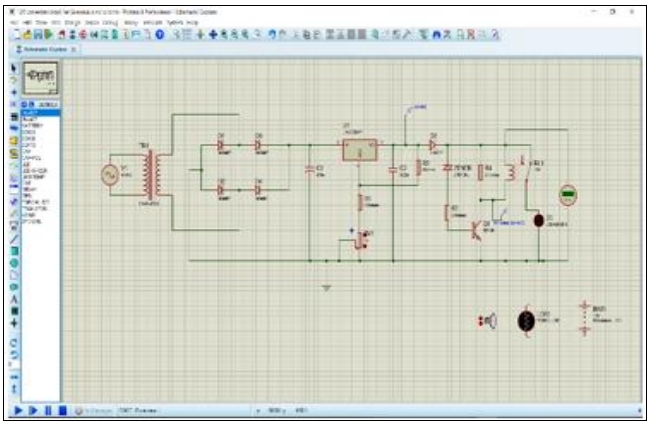

Fig 37: 12V AC-DC regulation circuit

The power conditioning system is built around a 12V converter circuit with an auto cut-off feature, designed using Proteus 8.17 software. This circuit is essential for transforming the variable AC voltage from the generator into a stable, regulated 12V DC supply while protecting the load from overvoltage and undervoltage conditions. The system begins with an AC source representing the turbine and generator, followed by a step-up transformer to elevate the low input voltage. A rectifier circuit then converts this AC to a pulsating DC, which is smoothed by a capacitor. A voltage regulator maintains a constant output, and a relay controlled by a Zener diode and transistor automatically disconnects the load if the voltage deviates from the safe 12V threshold, ensuring the entire system operates reliably and safely.

Components Summary Table

Table 2: Electronic components summary

Component	Function	Key Specification_Purpose
Transformer (TR1)	**Steps Up Voltage**	Boosts the turbine's low AC output voltage for effective processing.
Rectifier Circuit	**Converts AC to DC**	Four 1N4007 diodes convert AC to pulsating DC. Handles high voltage (1000V).
Smoothing Capacitor (C1)	**Reduces Ripple**	Smoothens the pulsating DC into a more stable voltage.
Voltage Regulator (LM317)	**Provides Stable Output**	Adjustable regulator (1.25V-37V) ensures a constant 12V output.
Resistors (R1, R2, RV1)	**Sets Output Voltage**	Two resistors set the base voltage; a variable resistor allows fine-tuning.
Output Capacitor (C2)	**Filters Noise**	Stabilizes the regulator's output by filtering residual noise.
Protection Diode (D6)	**Prevents Backflow**	1N4007 diode protects the circuit from reverse current.
Auto Cut-off Circuit	**Safety Switch**	**Zener Diode:** Senses overvoltage (>12V). **Transistor:** Amplifies signal to switch the relay. **Relay:** Physically disconnects the load to prevent damage.

Transformer (TR1)

Transformers either step up or step down the source voltage according to the circuit requirements. In this project, a step-up transformer was used to maximize the low voltage of the Savonius turbine. This is crucial for boosting the typically low voltage from the turbine to a level that is sufficient for effective rectification and regulation, thereby improving the overall system efficiency. A step-up transformer is a type of transformer that converts the low voltage (LV) and high current from the primary side of the transformer to the high voltage (HV) and low current value on the secondary side of the transformer. The reverse of this is known as a step-down transformer.

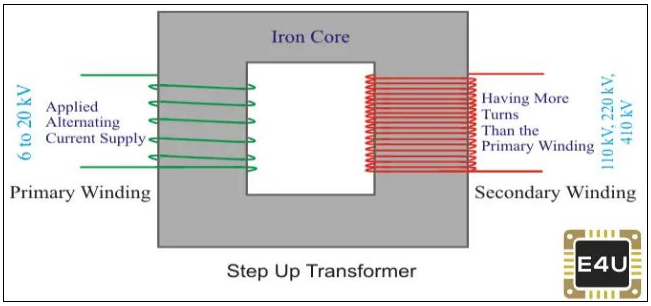

Fig 38: step-up transformer diagram

A transformer is static electrical equipment that converts electrical energy from the primary windings into magnetic energy in its core, then back to electrical energy on the secondary side. Step-up transformers are widely used in electrical systems and transmission lines. The operating frequency and nominal power are approximately equal on the primary and secondary transformer sides because the

transformer is a very efficient piece of equipment – while the voltage and current values are usually different. A transformer provides galvanic isolation in the electrical system. Due to these two main features, the transformer is the most important part of the electrical system and provides economical and reliable transmission and distribution of electrical energy. Transformers can transfer energy in both directions, from high voltage (HV) to low voltage (LV) and vice versa. This capability allows them to function as either step-up or step-down transformer, despite having the same design and construction.

The HV windings contain a huge number of turns compared with the LV windings. An LV winding wire has a bigger cross-section than HV wire because of the higher current value on the LV side. Usually, we place the LV windings close to the transformer core, and over them, we wound the HV windings.

The transformer turns ratio (n) for a step up transformer is approximately proportional to the voltage ratio:

$$n = \frac{V_P}{V_S} = \frac{N_P}{N_S}$$

Where $V_{P,S}$ are voltages, and $N_{P,S}$ are the turns numbers on the primary (LV) and secondary (HV) sides respectively. The primary side of a step-up transformer (LV side) has a smaller number of turns than the secondary side (HV side). That means energy flows from the LV to the HV side. The voltage is stepped up from the primary voltage (input voltage) to the secondary voltage (output voltage). This equation can be rearranged for the formula for the output voltage (i.e. secondary voltage). This is sometimes referred to as the step-up transformer formula:

$$V_S = \frac{N_S * V_P}{N_P}$$

The voltage value produced in energy generation is increased and prepared for use.

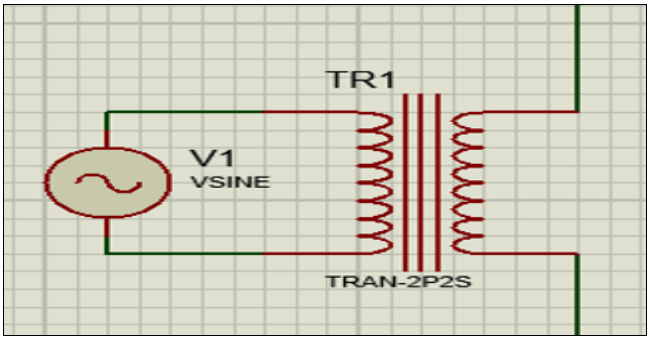

Fig 39: Transformer representation from Proteus 8.17

Fig 40: Actual transformer

Rectifier Circuit

Made from four diodes, each diode prevents voltage from returning backwards to the source, therefore enabling the conversion of AC voltage to DC. A specific diode, the 1N4007, is used. The 1N4007 is a silicon rectifier diode known for its ability to handle high reverse voltages up to 1000V, making it ideal for various electronic applications, particularly in power rectification. The output of the rectifier circuit will be a pulsating DC voltage. The rectifier is fundamental as it converts the generator's alternating current into direct current, which is necessary for charging batteries and powering DC loads like LED lights. The 1N4007 diodes are vital for their durability and high voltage tolerance, ensuring the circuit's reliability.

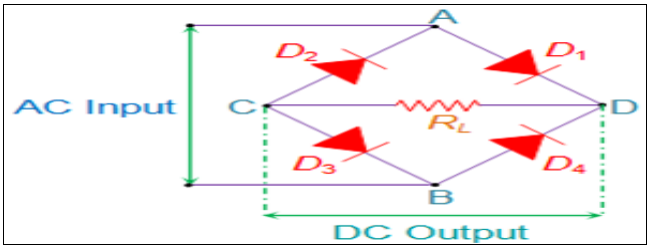

Fig 41: Full-wave bridge rectifier diagram

When a positive pulse appears at the AC input (terminal A is positive, terminal B is negative), diodes D1 and D3 become forward biased, while diodes D2 and D4 are reverse biased. As a result, the current flows along the short-circuited path created by the diodes D1 and D3 (considering the diodes to be ideal). Therefore, the voltage developed across the load resistor RL will be positive towards the end connected to terminal D and negative at the end connected to the terminal C.

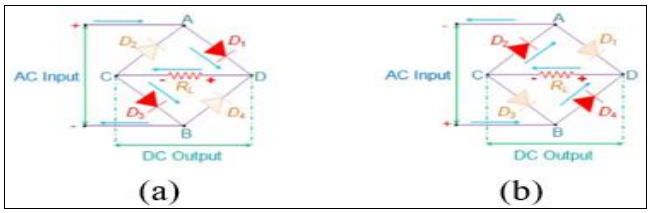

Fig 42: Current through the bridge rectifier (a) positive half cycle (b) negative half cycle

When a negative pulse appears at the AC input (terminal A is negative, terminal B is positive), diodes D2 and D4 become forward biased, while diodes D1 and D3 are reverse biased. It is important to note that the voltage across RL remains the same polarity regardless of whether the AC input pulse is positive or negative. Thus, the output of the bridge rectifier always has the same polarity, as shown by the waveforms;

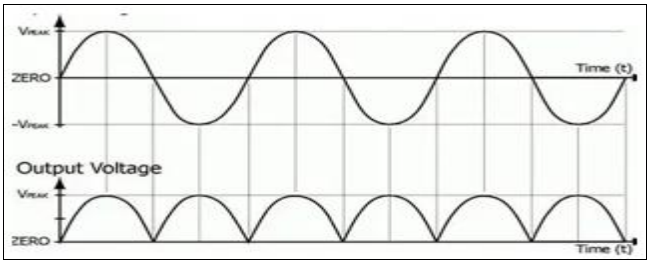

Fig 43: Input- output waveforms of a rectifier

However, it is to be noted that the bridge rectifier's DC will be pulsating in nature. In order to obtain a pure form of DC, one has to use a capacitor in conjunction with the bridge circuit.

Bridge rectifiers for a particular application are selected by considering the load current requirements. These bridge rectifiers are quite advantageous as they can be constructed with or without a transformer and are suitable for high voltage applications.

Types of Bridge Rectifiers

The bridge rectifier just discussed is a single-phase type, however, it can also be extended to a three-phase rectifier. These two types can be further classified into full controlled, half controlled, or uncontrolled bridge rectifiers. The circuit that we just discussed is uncontrolled since we cannot control the biasing of the diode, but if all the four diodes are replaced with a thyristor, its biasing can be controlled by controlling its firing angle via its gate signal. It results in a fully controlled bridge rectifier. In a half controlled bridge rectifier, half of the circuit contains diodes, and the other half has thyristors.

1N4007 diode

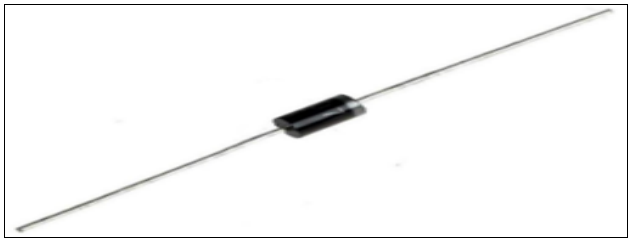

Fig 44: 1N4007 diode

A diode is a basic PN junction semiconductor device. Because it is constructed with P and N-type materials. It acts as a one-way switch that allows the current to flow in one direction and halts in the other direction.

1N4007 belongs to the silicon family of1N400X series. It is a general-purpose rectifying diode that serves its purpose of converting alternating current signals (AC) to direct current signals (DC) in electronic products. It has two terminals, Anode (positively-charged) and Cathode (negatively-charged).

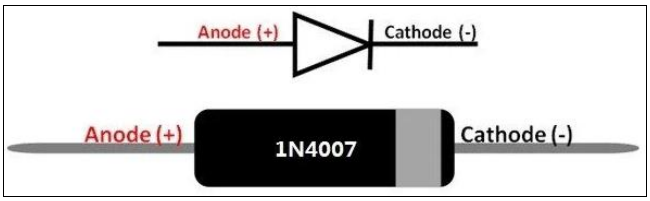

Fig 45: 1N4007 diode diagram

For the current to flow from anode to cathode, the anode should be connected to a higher potential than the cathode (forward biasing). The current which flows from anode to a cathode terminal is known as a forward current. Reverse biasing will restrict the flow of current and can damage the device if voltage applied is greater than reverse breakdown voltage. During reverse biasing a leakage current flow through a diode which is negligible compared to forward current.

When the input voltage applied to the anode terminal is positive (+ve) as compared to the cathode terminal, the diode is said to be forward-biased. When this applied input voltage becomes greater than 0.6 volts, IN4007 diode acts as a short circuit.

In the context of the research paper by (Nanda and Sarangi, 1997), the 1N4007 was not selected for a specific circuit application but rather as a representative and widely available commercial silicon p-n junction diode. The authors used it as a model system to study fundamental semiconductor properties, such as the temperature dependence of forward voltage and capacitance, which are critical for applications in diode thermometry and junction characterization. Like any other diode, the 1N4007 requires a reverse recovery time to recover during switching from forward to reverse biased mode. During reverse recovery, diode produces a high reverse current which produces heat. The higher is a frequency of input signal, the higher time diode takes to recover its state. 1N4007 is a low-frequency diode due to high recovery time. Therefore, the 1N4007 should be used for low frequency applications only.

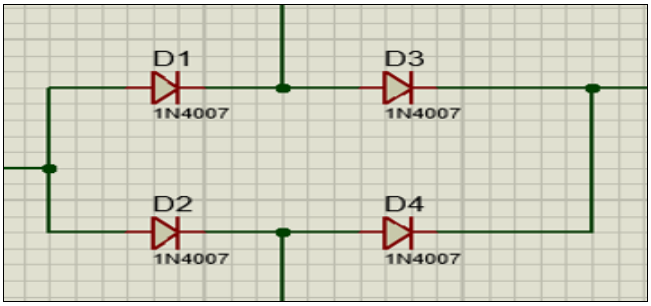

Fig 46: Rectifier circuit from four (4) 1N4007 diode proteus 8.17 version

Smoothing Capacitor (C1)

The primary function of this capacitor is to smoothen the pulsating voltage from the rectifier circuit. This component is critical for reducing the voltage ripple, resulting in a more stable DC voltage that is suitable for sensitive electronic components and for providing consistent power to the load. A smoothing capacitor plays a crucial role in maintaining stable performance, especially in power supplies. Power supplies often generate unwanted ripple voltage due to the nature of alternating current (AC) to direct current (DC) conversion. To ensure that electronic devices operate smoothly, a smoothing capacitor helps to filter out these ripples, providing clean and steady voltage.

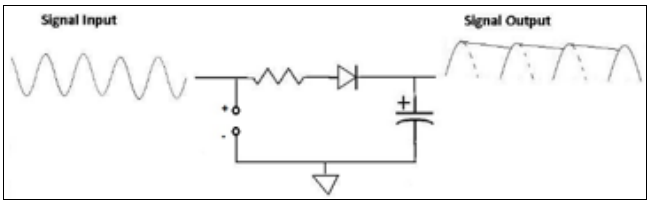

Fig 47: Capacitor circuit diagram

A smoothing capacitor is a type of electrolytic capacitor typically used in power supply circuits to reduce the ripple in DC voltage. When AC voltage is converted to DC, the resulting voltage often fluctuates, creating a ripple effect. Smoothing capacitors are designed to smooth out these fluctuations by storing charge during high voltage periods

and releasing it during low voltage periods. This results in a more stable and continuous flow of current to the components in a circuit, which is essential for the proper operation of many electronic devices.

The capacitor's ability to smooth is based on its charge and discharge cycle. The capacitor charges when the input voltage rises above its voltage level, and it discharges when the input voltage falls below it. This action helps fill in the gaps created by the fluctuating voltage, providing a much more consistent DC output. If the DC voltage contains ripples or fluctuations, it can cause erratic behavior, reduce the efficiency of the device, or even lead to component failure. By reducing ripple voltage, smoothing capacitors ensure that sensitive components in a circuit receive a consistent voltage. This prevents potential issues such as overheating, distortion, or malfunction, which can be costly to repair. In high-performance circuits, the smoothness of the power supply can directly impact the overall performance and reliability of the device.

How Smoothing Capacitors Reduce Ripple Voltage

Ripple voltage is the unwanted alternating component that remains after AC voltage is converted to DC. In a typical rectifier circuit, the rectifier converts AC to DC, but the output is not a smooth DC signal. This is where the smoothing capacitor comes into play.

When the AC voltage is rectified, it produces a pulsating DC signal with peaks and valleys. The smoothing capacitor works by charging up during the peak of the voltage and discharging during the valley. This helps fill in the gaps between the peaks, making the voltage more uniform and steadier. The size and capacitance of the capacitor determine how effectively it can smooth the voltage; larger capacitors with higher capacitance values can store more energy and filter out more ripple.

Fig 48: Polarized smoothing capacitor

Voltage Regulator (LM317EMP)

The LM317EMP is a three-terminal and adjustable positive voltage regulator that supplies above 1.5A of current over a voltage range from 1.25V to 37V. This type of voltage regulator is very simple to use and needs only two external resistors to set the output voltage. Its role is to provide a constant, precise output voltage regardless of fluctuations in the input voltage or load current, which is essential for protecting the load from damage and ensuring consistent in output voltage. The input pin, output pin, and adjustment pin are the three terminals. The LM317 circuit diagram shown below is a typical configuration of the LM317 voltage regulator circuit diagram, which includes the decoupling capacitors. A low-side and high-side resistor are connected in series to form a resistive voltage divider, which is a passive linear circuit used to produce an output voltage that is a fraction of its input voltage.

Because the LM317 regulator can provide excess output current, it is conceptually considered an operational amplifier. The adjustment pin is the amplifier's inverting input, and an internal bandgap reference voltage is used to set the non-inverting input to produce a stable reference voltage of 1.25V.

A resistive voltage divider between the output and ground can be used to continuously adjust the output pin voltage to a fixed amount, converting the operational amplifier to a non-inverting amplifier. A bandgap reference voltage is used to produce constant output voltage regardless of supply power changes. It is also known as a temperature-independent reference voltage, and it is commonly used in integrated circuits.

The output voltage of the LM317 voltage regulator circuit (ideally):

$$V_{out} = (1+ (RL/RH)) \times V_{ref}$$

Because some quiescent current flows from the device's adjustment pin, an error term is added.

$$V_{out} = (1+(RL/RH)) \times V_{ref} + IQR$$

The LM317 voltage regulator circuit diagram is designed to achieve a more stable output by keeping the quiescent current less than or equal to 100 micro-Ampere. As a result, the error can be ignored in all practical cases. If we substitute the load for the low-side resistor of the divider in the LM317 voltage regulator circuit diagram, the resulting configuration of the LM317 regulator will regulate the current to a load. As a result, this LM317 circuit can be referred to as the LM317 Current Regulator Circuit.

The output current is the voltage drop of the reference voltage across the resistance RH and is given as:

$$I_{out} = V_{ref}/RH$$

In the ideal case. Taking the quiescent current into account, the output current is given as:

$$I_{out} = (V_{ref}/RH) + IQ.$$

The LM317 and LM337 linear voltage regulators are frequently used in DC-DC converter applications. Linear regulators are designed to draw as much current as they supply. The power generated by multiplying this current by the voltage difference between the input and output is dissipated and wasted as heat.

As a result, heat must be considered for significant design, which leads to inefficiency. When the voltage difference increases, so do the power wasted, and this dissipated waste power can sometimes exceed the supplied power. Even though this is insignificant, we must accept this trade-off because linear voltage regulators with a few additional components are a simple way to obtain stable voltage. Switching voltage regulators are an alternative to linear regulators because they are generally more efficient, but they require more components to design and thus take up more space.

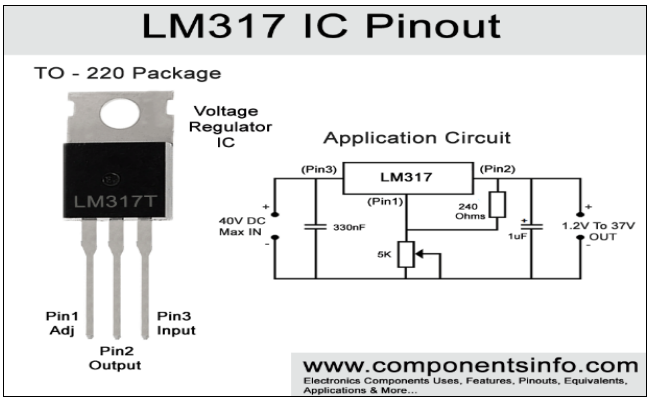

Fig 49: Voltage regulator LM317 and its equivalent circuit

Resistors R1 and R2

The voltage regulator works on the principle of two resistors to maintain a constant output voltage. A variable resistor (RV1) is added to allow for fine-tuning of the output voltage and to prevent damage to the LM317EMP IC. These resistors are key to setting and stabilizing the desired 12V output, while the variable resistor provides crucial adjustability to calibrate the system accurately under different operating conditions.

Fig 50: Resistors

A resistor is a passive two-terminal electrical component that limits the current flowing in electrical or electronic circuits. Its property to resist the flow of current is called resistance, expressed in ohm (Ω), named after German physicist Georg Simon Ohm. Resistors are available in different sizes. Its size is directly proportional to its power rating. The power rating is the maximum amount of power that a resistor can dissipate without being damaged by excessive heat build-up. The larger the surface area covered by a resistor, the more power it can dissipate.

Types of Resistors

There are two different types of resistors:

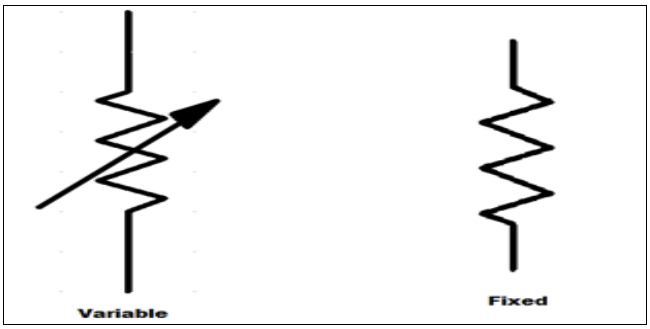

Fig 51: Resistor symbols of types of resistors

Fixed resistors are designed to set the right conditions in a circuit. Their values should never be changed to adjust the circuit since those were determined during the design phase. It can have a carbon composition or chip-and-wire wound type. It can also be made with a mixture of finely ground carbon or be very small in size and for high power rating.

Variable resistors have fixed resistor elements plus a slider. The slider taps onto the main resistor element so there will be three connections; two are connected to the third element and one to the slider. Examples of this are potentiometers, rheostats and trimmers.

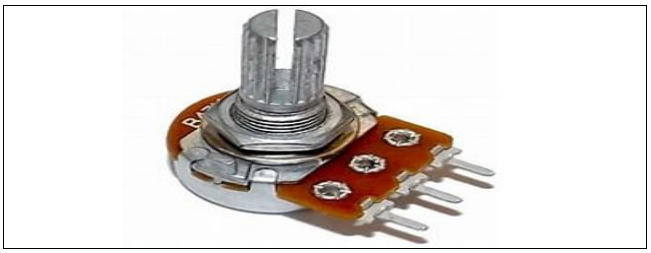

Fig 52: Potentiometer

How Resistors Work

Wiring a resistor in a circuit will reduce the current by a precise amount. Resistors from the outside, look the same. However, there is an insulating ceramic rod running through the middle with copper wire wrapped around the outside. Resistance depends on those copper turns. The thinner the copper, the higher the resistance since it is hard for the electrons to pass through it. It is easier for the electrons to flow in some conductor materials than insulators.

George Ohm studied the relationship between resistance and the size of the material that was used to make the resistor. He proved that the resistance (R) of a material increases as its length increases. This means that longer and thinner wires offer more resistance. On the other hand, resistance decreases as the thickness of wires increases.

Resistor Color Codes

The chart below shows how to determine the resistance and tolerance for resistors. The table can also be used to specify the color of the bands when the values are known. An automatic resistor calculator can be used to quickly find the resistor values.

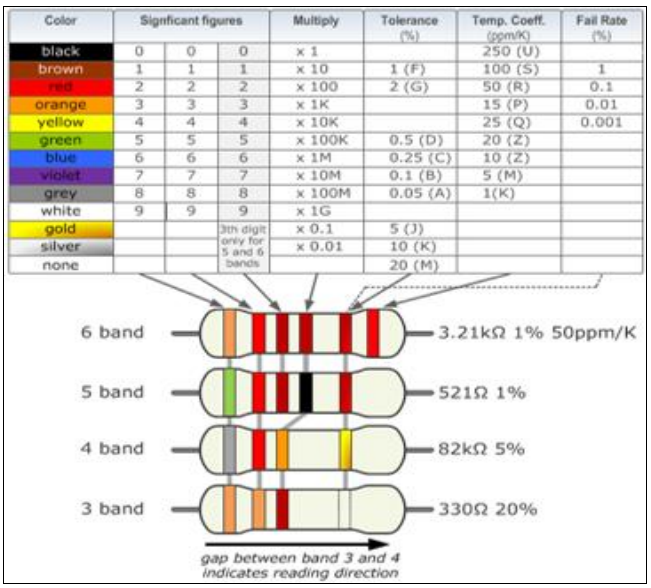

Fig 53: Chart for different resistor color codes

Capacitor C2

This capacitor is placed at the output of the regulator to stabilize the output voltage further. It enhances the regulator's performance by filtering out any residual noise or transient fluctuations, ensuring a clean and stable DC supply to the load.

Fig 54: Capacitor

Diode D6 (1N4007)

This diode, identical to those in the rectifier, is placed at the output to prevent backflow of current from the load towards the regulator. This feature protects the sensitive voltage regulator and other upstream components from potential damage caused by reverse current, such as from a battery when the turbine is not spinning.

Auto Cut-off Arrangement (Zener diode, resistors, transistor switch, and relay)

Zener Diode (ZPD12RL)

It operates based on a voltage-triggered breakdown that allows it to conduct electricity in reverse, providing a stable voltage reference. In this project, the zener diode starts to conduct when the voltage goes above 12V. It acts as the voltage-sensing element, triggering the protection circuit when a dangerous overvoltage condition is detected.

Zener Diode Working Principle

When a PN junction diode is reverse biased, the depletion layer widens. Continuously increasing the reverse bias voltage across the diode makes this layer even wider. Simultaneously, a constant reverse saturation current flows due to minority carriers. At a specific reverse voltage, minority carriers gain enough kinetic energy from the strong electric field. These energetic electrons collide with stationary ions in the depletion layer, releasing more electrons. The process continues, generating additional free electrons through cumulative collisions. Due to this commutative phenomenon, very soon, huge free electrons get created in the depletion layer, and the entire diode will become conductive. This type of breakdown of the depletion layer is known as avalanche breakdown.

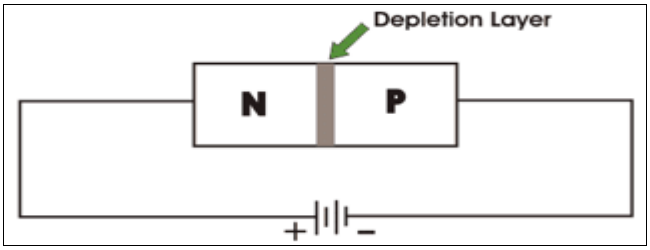

Fig 55: Zener diode circuit diagram

This cumulative effect quickly generates numerous free electrons in the depletion layer, making the diode conductive. This process, known as avalanche breakdown, does not have a sharp onset. There is another type of breakdown in depletion layer which is sharper compared to avalanche breakdown, and this is called Zener breakdown. When a PN junction is diode is highly doped, the concentration of impurity atoms will be high in the crystal. This higher concentration of impurity atoms causes the higher concentration of ions in the depletion layer hence for same applied reverse biased voltage, the width of the depletion layer becomes thinner than that in a normally doped diode.

The thinner depletion layer causes a high voltage gradient or electric field strength. Increasing the reverse voltage further leads to a point where electrons break free from covalent bonds, making the region conductive. This is the Zener breakdown. The voltage at which this breakdown occurs is called Zener voltage. If the applied reverse voltage across the diode is more than Zener voltage, the diode provides a conductive path to the current through it hence, there is no chance of further avalanche breakdown in it. Theoretically, Zener breakdown occurs at a lower voltage level then avalanche breakdown in a diode, especially doped for Zener breakdown. The Zener breakdown is much sharper than avalanche breakdown. The Zener voltage of the diode gets adjusted during manufacturing with the help of required and proper doping. When a zener diode is connected across a voltage source, and the source voltage is more than Zener voltage, the voltage across a Zener diode remains fixed irrespective of the source voltage.

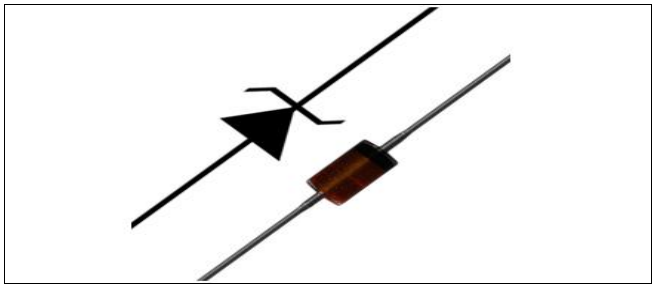

Fig 56: Zener diode symbol and image

NPN Transistor switch

The NPN transistor acts as a gated device for electric current. The input signal from the Zener diode controls this gate. When the Zener diode conducts (at or above 12V), the transistor receives current and starts conducting, simultaneously amplifying the signal to compensate for voltage drops. The transistor serves as a robust electronic switch that can handle the current required to activate the relay based on the small signal from the Zener diode.

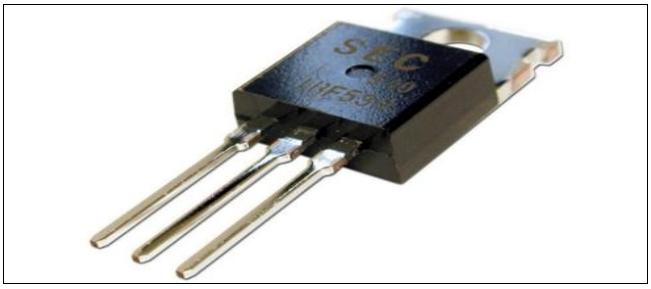

Fig 57: NPN transistor switch

NPN Transistor Working Principle

An NPN transistor is the most commonly used bipolar junction transistor, and is constructed by sandwiching a P-type semiconductor between two N-type semiconductors. An NPN transistor has three terminals– a collector, emitter and base. The NPN transistor behaves like two PN junctions diodes connected back to back.

These back-to-back PN junction diodes are known as the collector-base junction and base-emitter junction.

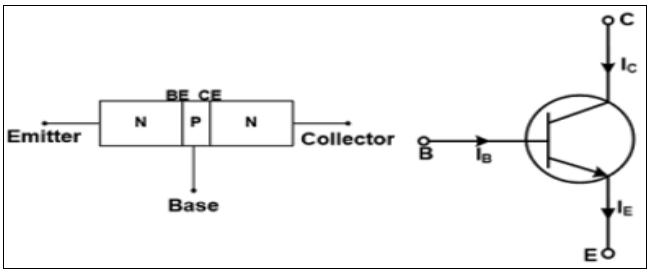

Fig 58: NPN transistor diagram

The base-emitter junction is forward bias condition by the supply voltage V_{EE}, while the collector-base junction is reverse biased by the supply voltage V_{CC}.

In forward bias condition, the negative terminal of supply source (V_{EE}) is connected to the N-type semiconductor (Emitter). Similarly, in a reverse bias condition, the positive terminal of the supply source (VCC) is connected to the N-type semiconductor (Collector). The depletion region of the emitter-base region is thin compared to the depletion region of the collector-base junction (Note that the depletion region is a region where no mobile charge carriers are present and it behaves like a barrier that opposes the flow of the current).

In N-type emitter, the majority charge carrier is electrons. Therefore, electrons start flowing from N-type emitter to a P-type base. And because of electrons, the current will start flowing the emitter-base junction. This current is known as emitter current I_E. Electrons move into the base, a thin, lightly doped P-type semiconductor with limited holes for recombination. Therefore, most electrons bypass the base, with only a few recombining. Because of the recombination, the current will flow through the circuit and this current is known as base current I_B. The base current is very small compared to the emitter current. Typically, it is 2-5% of the total emitter current. Most of the electrons pass the depletion region of a collector-base junction and pass through the collector region. The current flowing by the remaining electrons is known as the collector current IC. The collector current is large compared to the base current.

The transistor operates on different modes or regions depends on the biasing of junctions. It has three modes of operation: cut-off mode, saturation mode and active mode:

Cut-off Mode: In cur-off mode, both junctions are in reverse bias. In this mode, the transistor behaves as an open circuit. And it will not allow the current to flow through the device.

Saturation Mode: In the saturation mode of a transistor, both junctions are connected in forward bias. The transistor behaves as a close circuit and current flow from collector to emitter when the base-emitter voltage is high.

Active Mode: In this mode of a transistor, the base-emitter junction is forward bias and collector-base junction is reverse biased. In this mode, the transistor operates as a current amplifier.

The transistor operates as switched ON in saturation mode and switched OFF in cut-off mode. When both junctions are connected in the forward bias condition and sufficient voltage is given to input voltage. In this condition, collector-emitter voltage is near to zero and the transistor operates as a short circuit. In this condition, the current will start flowing between collector and emitter.

When both junctions are connected in reverse bias, the transistor behaves as an open circuit or OFF switch. In this condition, the input voltage or the base voltage is zero. Therefore, the entire Vcc voltage appears across the collector. But, because of the reverse bias of the collector-emitter region, the current cannot flow through the device. Hence, it behaves as an OFF switch.

Relay

A relay is an electrically operated switch. When the voltage exceeds 12V, the energized relay coil will open its contacts, isolating the load from the entire circuit. The same applies for undervoltage. This is the final safety mechanism that physically disconnects the load during fault conditions, directly protecting it from damage due to overvoltage or undervoltage.

Relay Working Principle

A relay is an electrically controlled switching device. It consists of an electromagnet and a set of contacts that open or close when voltage is applied to the electromagnet. They are basically classified into two types based on their working principle as electro-mechanical and solid-state relays.

Electromechanical relays transfer signals between its contact through a mechanical motion. It consists of two sections: the first is the electromagnet section and the other is the armature and mechanical contacts section. The electromagnet section consists of a set of coil wound over a magnetic core. When an input voltage (almost equal to the rated voltage of the coil) is applied to the coil, it gets magnetized and attracts the armature. The mechanical contacts are attached to the armature. Hence, when the armature is pulled towards the electromagnet, the contact closes. When the input voltage applied to the coil is removed, the armature is brought back to its original position by the spring release.

Solid-state relays are commonly known as SSRs. Unlike electromechanical type, they do not possess any mechanically moving parts. On the other hand, it consists of semiconductor and electronic components within. In solid-state relays, the electromagnetic section is replaced by optocoupler and required driver circuits and the output contact section is replaced by a TRIAC or transistor plus snubber and driver circuits.

When the rated voltage is applied to the input section, current flows through the optocoupler. The output of the optocoupler is used to operate the switching circuit of TRIAC or transistor. Switching circuit applies a gate pulse to the TRIAC and the TRIAC starts conducting. Similarly, when the applied input voltage is removed, the optocoupler turns off the TRIAC switching circuit and which, in turn, stops the gate pulse to the TRIAC and the TRAIC stops conducting.

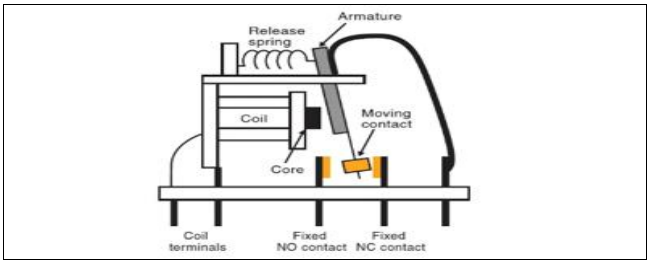

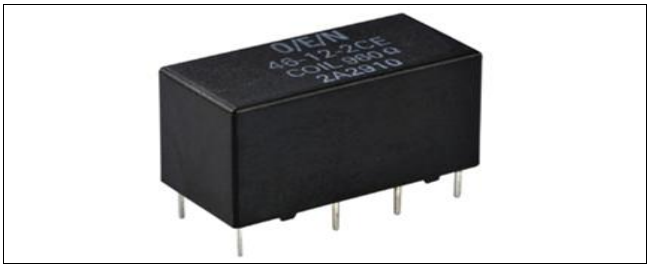

Fig 59: Standard 12V electromechanical relay

3.5 Budget

Table 3: Budget for the entire project

Item	Description	Unit price (K)	Amount (K)
1	PVC tube x 1	70	70
2	Bearings x 2	80	160
3	Mounting x 1	100	100
4	Motor x 1	350	350
5	Gear system x 1	30	30
6	Transformer – step-up x 1	250	250
7	Diodes **(Zener x 1, 1n4007 x5)**	5	30
8	Resistors x 4	2	8
9	Variable resistor x 1	5	5
10	Capacitor x 2	15	30
11	Relay x 1	50	50
12	LED green x 1	5	5
13	Transistor x 1	15	15
14	LED lightbulb x 1	50	50
15	Araldite glue x 1	20	20
		Total	**K1,173**

4. Results

4.1 Overview

This chapter presents the findings from the experimental testing and performance evaluation of the developed mini Savonius wind turbine prototype. The results are systematically presented to address the specific research objectives, detailing the outcomes of the turbine's operation under controlled conditions. Key performance metrics, including voltage output, and power generation, are analyzed and discussed. Furthermore, this chapter interprets the data in the context of the project's viability targets, particularly the ability to power a standard LED streetlight, and links the findings to the broader research gaps identified in the literature. The discussion section contextualizes these results, explaining their significance and how they contribute to the field of urban wind harvesting in developing regions.

4.2 Baseline Study Results

The global shift toward sustainable energy is driving innovation in urban power generation. This study examines the potential for integrating small-scale wind energy systems into the Munali Flyover Bridge in Lusaka, Zambia. To assess feasibility, a clear technical baseline must be established, founded upon two key considerations: the anticipated energy output from the selected wind turbine design, and the specific structural and environmental conditions of the bridge itself.

A vertical-axis turbine design is proposed for its adaptability to shifting wind directions and its operational suitability for a bridge setting. The energy potential of this system is intrinsically linked to the unique context of the flyover, including its elevated height, the aerodynamic influence of its design, and the additional wind generated by vehicular traffic. By evaluating the turbine's performance within this specific environment, this baseline study aims to provide a realistic estimate of energy production. This foundational assessment will guide further analysis on practical integration, viability, and safety, exploring how the bridge might serve a dual role in transportation and local renewable energy generation.

Wind energy generation formula

According to Johnson *et al*. (2006) [15], the total kinetic energy power contained in the wind passing through a given area is given by;

$$P_{\text{wind}} = \frac{1}{2}\rho A v^3$$

Where:

P_{wind} = **Power available in the wind** (Watts, W).

ρ (rho) = **Air density** (kg/m³). This varies with temperature and altitude.

A = **Rotor swept area** (m²). For a horizontal-axis turbine, this is the area of the circle the blades sweep: $A=\pi R^2$, where R is the rotor radius.

V = **Wind speed** (m/s).

Based on the International Standard Atmosphere (ISA) model, the standard air density at sea level is typically taken as 1.225 kg/m³. However, site-specific measurements from Zambia's wind resource assessment indicate that air density can vary significantly with elevation and local conditions. For example, at the Lusaka measurement site, the average air density at hub height (130 m) was reported as 1.03 kg/m³, with the average wind speed of 8.0 m/s (Renewable Energy Wind Mapping for Zambia: 24-month Site Resource Report, 2019).

Expected Wind Energy from the Rotor

Rotor parameters;

Height = 25cm = 0.25m

Diameter = 26cm = 0.26m

Swept area = $A=\pi R^2$

$A = \pi (0.13)^2 = 0.0169 m^2$

Calculating wind power (Pwind)

$$P_{\text{wind}} = \frac{1}{2}\rho A v^3$$

$P_{wind} = ½ (1.03kg/m^3) (0.0169m^2) (8.0m/s)^3$

$P_{wind} = 4.456W$

Wind power according to the rotor design is **4.456W**.

Munali Flyover Bridge

The Munali Flyover Bridge in Lusaka, Zambia, is a key piece of infrastructure designed to ease traffic congestion and improve connectivity. As part of broader urban and transport development efforts to support economic growth, enhance road safety, and accommodate increasing vehicular traffic in Zambia's capital, this flyover represents a significant investment in modernizing the city's road network and facilitating smoother movement of people and goods. Its elevated structure, clear surrounding space, and consistent high-speed vehicle traffic also make it an ideal site for testing the operation of a mini Savonius wind turbine, taking advantage of the uninterrupted airflow and traffic-induced wind currents generated along its span.

Fig 60: Arial view of Munali flyover bridge

According to the Spannovation Group, Lusaka City Decongestion Project Report backed by Road Develpment Agency (RDA), here are the bridge parameters;

Table 4: Muali flyover bridge specifications

Superstructure	Girders
Type: Composite Steel (Steel Girders with Concrete Deck)	**Type:** Six lines of straight plate girders
Span Arrangement: Three Simply Supported Spans (31m + 40m + 40m)	**Spacing:** 2.5 meters
Total Length: Approximately 111 meters	**Girder Depths:** 1.7 meters for the 31m span, 2.1 meters for the 40m spans
Radius of Curvature: 2000m (mild plan curvature)	**Pier Type:** Two-pier portal arrangement
Deck Width: 14.6 meters	**Pier Cap**: Hammerhead type
Deck Slab: 225mm thick, Cast-in-Place	**Foundation:** Open Foundation
Traffic Lanes: 4 lanes, separated by a 0.6m wide central crash barrier	

4.3 System Implementation Results

The data collection process involved a preliminary assessment of the wind energy potential using a road survey to determine baseline viability. Due to the unavailability of a commercial anemometer, wind speed was correlated to the electrical output, with a small DC motor functioning as a generator. This indirect method relies on the direct relationship between the rotational speed of a rotor and the wind speed acting upon it.

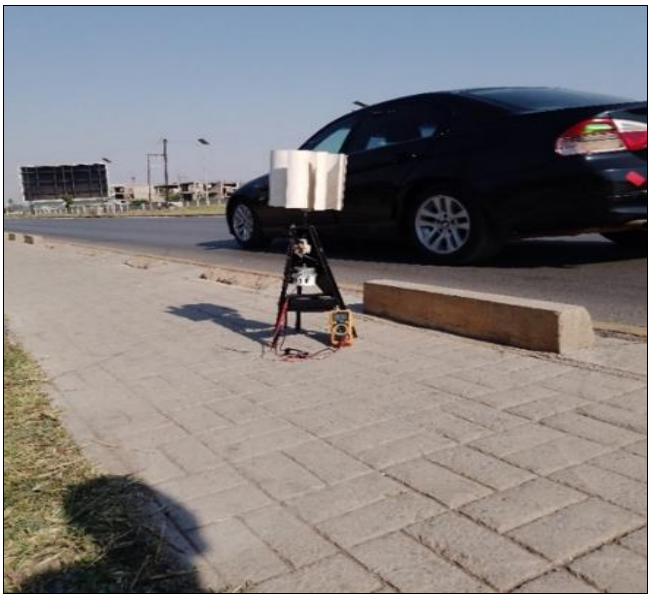

Fig 61: Turbine testing along Nangwenya road, Lusaka, Zambia

A digital multimeter was used to measure the voltage output from this motor-generator setup. By analyzing these electrical readings, an estimate of the available wind voltage was established to inform the initial design requirements for the Savonius turbine prototype. This approach confirmed that the locally available wind resource was sufficient to warrant the turbine's development.

Survey Results

Table 5: Survey Results

Measurement position	Image of highest reading	Recorded voltage (V)	Recorded current (I)	Average power (W)
Road survey (ground)		0.531, 0.537, 0.662, 0.514, 0.616, 0.511, 0.579, 0.509, 0.488, 0.657 **0.560V**	1.62 1.77 2.74 2.19 2.22 2.02 2.08 2.04 2.01 1.51 **2.02A**	**1.131W**
Road survey (1m above ground)		0.74 0.89 0.90 0.82 0.90 1.12 1.02 0.93 0.84 0.98 **0.914V**	4.01 3.74 4.29 4.19 5.68 4.47 4.71 4.29 4.40 4.94 **4.47A**	
Average				**4.09W**

The Circuit

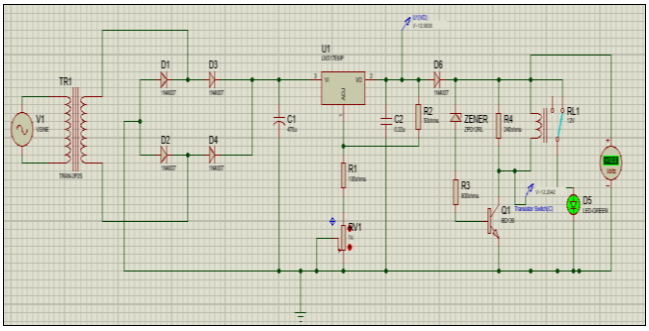

Fig 62: Circuit design using Proteus 8.17

The final system testing and validation phase confirmed the operational efficacy of the electronic power conditioning subsystem. The circuit design, modeled and refined in Proteus 8.17 simulation software, was successfully transitioned to physical hardware.

The core voltage regulation module demonstrated the performance by accepting a low input voltage of 3VDC and, through the integrated step-up transformer and adjustable feedback network based on an LM317 regulator, producing a stable and precisely controllable output of 12VDC. Furthermore, the design's flexibility was validated by using the variable resistor (RV1) to tune the output up to a maximum of 14VDC, confirming the circuit's wide dynamic range and adherence to design specifications for adjustable regulation.

For comprehensive hardware validation under high-power conditions, the circuit was subjected to a mains-powered test. A step-down isolation transformer (230VAC/12VAC) provided a safe and controlled AC input, simulating a high-current source. The physical circuit successfully rectified, filtered, and regulated this input, producing a DC output voltage ranging from 14.0 VDC to 19.5 VDC. This result, which aligns with the theoretical calculations and simulation predictions, conclusively verifies the circuit's functionality, stability, and readiness for integration with the turbine's generator in the final prototype assembly.

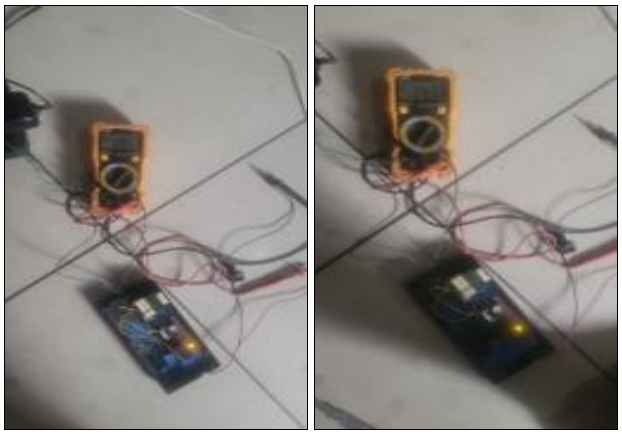

(a) (b)

Fig 63: Physical circuit measurements (a) showing regulated lowest voltage from mains (b) showing the highest regulated voltage

4.4 Data Analysis

A field survey was conducted along Nangwenya Road, a dual-carriageway behind the University of Zambia, selected for its clear, straight sections that permit fast-moving vehicle traffic. The objective was to empirically characterize the wind energy potential generated by vehicular movement. The survey methodology involved measuring the electrical output of a small, calibrated DC motor functioning as a turbine-generator. A digital multimeter was used to record the open-circuit voltage, providing a direct proxy for wind speed and kinetic energy. Measurements were systematically taken at two distinct heights at ground level and one meter above ground; to analyze the variation in wind resource with elevation.

Key Findings from the Field Survey

The analysis of the collected voltage data revealed several critical insights:

1. Correlation with Vehicle Characteristics: A strong positive correlation was observed between the generated voltage and the size and speed of passing vehicles. Larger vehicles, such as trucks and buses, consistently induced significantly higher voltage spikes due to their greater displacement of air. Similarly, faster-moving vehicles generated a more pronounced and sustained wind wake compared to slower traffic. Conversely, small sedans and slow-moving vehicles produced minimal, often negligible, electrical output.

2. Effect of Turbine Elevation: The data conclusively demonstrated the importance of turbine placement height. The average voltage recorded at 1 meter above ground (0.914 V) was approximately 63% higher than the average at ground level (0.560 V), as detailed in Table 4.1. This confirms that elevating the turbine rotor is essential to capture stronger and more consistent wind currents above the ground-level boundary layer.

3. Mechanical System Performance: The prototype's mechanical components, including the multi-blade Savonius rotor and the simple gear system, demonstrated smooth starting and stable operation in the variable wind conditions. The rotor responded effectively to gusts from different directions, validating its omnidirectional design principle.

Identified Challenges and Project Limitations

The survey and development process highlighted significant practical challenges:

Equipment Constraints: The project was hampered by a lack of specialized measurement equipment, specifically a commercial anemometer for direct wind speed measurement and a data logger for capturing high-frequency fluctuations.

Component Scarcity: Sourcing electronic components locally proved difficult. A critical limitation was the inability to acquire a efficient, low-voltage step-up transformer capable of boosting the generator's low output (often as low as 2V) to a usable level for the 12V circuit.

Mechanical Limitations: The available 3:1 gear ratio was insufficient to amplify the turbine's low rotational speed to a level where the generator could produce adequate voltage. A higher-ratio gearbox (e.g., 10:1) was identified as a necessity but was not locally available.

Primary Failure Mode: The core failure of the initial prototype was its inability to generate sufficient voltage to activate the 12V regulation circuit. The combination of low rotational speed from the turbine and an insufficient gear ratio resulted in a generator output that consistently remained below the operational threshold of the power conditioning system.

Logistical Note: Direct measurement and testing on a flyover bridge required official safety permits and the presence of traffic officers, a process that could not be finalized within the project timeline.

Recommendations and Future Upgrades

Based on the findings and challenges of this survey, the following upgrades are critically recommended for future iterations:

Enhanced Gear System: The most immediate upgrade is the implementation of a higher-ratio gear system (10:1 or greater). This will directly address the voltage generation issue by significantly increasing the input RPM to the generator.

Expanded Site Surveys: Future data collection should be expanded to include a wider variety of environments to comprehensively map the urban wind resource. Key locations include:

Flyover bridges to capitalize on the "piston effect."

High-speed highways with consistent heavy vehicle traffic.

The rooftops of tall buildings to assess ambient wind resource potential.

Generator and Circuit Optimization: Explore the use of more sensitive, low-RPM permanent magnet generators and specialized power management circuits, such as boost converters, designed to efficiently handle very low input voltages.

5. Discussion and Conclusion

5.1 Introduction

This chapter synthesizes the findings from the design, development, and testing of the mini Savonius wind turbine system for flyover bridges. It discusses the outcomes in relation to the initial research gaps, evaluates the system's effectiveness, compares it with similar works, and outlines its potential applications and future improvements, with a specific focus on relevance for Zambia and similar developing regions.

5.2 Discussion

The project successfully demonstrated the feasibility of generating usable electricity from vehicle-induced wind on flyover bridges using a simple, cost-effective system. The core achievement lies in addressing the application gap for small-scale, direct infrastructure power. The system's design, prioritizing high starting torque and low-wind-speed operation over peak efficiency, proved critical for harnessing the intermittent gusts from traffic. Furthermore, the use of locally available PVC material and a straightforward electrical circuit directly confronts the techno-economic viability gap, presenting a model that is financially and technically accessible for developing nations, unlike many complex, cost-prohibitive systems found in the literature.

5.2.1 The Baseline Study

The baseline study, conducted from a residential rooftop using a DC motor and a digital multimeter, confirmed the presence of a viable wind resource even in non-ideal locations. This low-fidelity approach was a practical necessity that underscored a key finding: the energy potential, while modest, is sufficient for targeted applications like LED street lighting. This phase successfully established the foundational performance target, to power a 12V LED system—justifying the subsequent design focus on reliability and cost-effectiveness over raw power output.

5.2.2 Use of Technology

The technology stack was deliberately selected for its appropriateness to the context. The multi-blade, PVC Savonius rotor provided the necessary self-starting capability and durability. The 3:1 gear system effectively amplified the low rotational speeds to a range suitable for the generator. The 12V converter circuit with auto cut-off was the cornerstone of the system's practicality, ensuring stable power delivery and protecting the load from voltage fluctuations, a common and often unaddressed challenge in real-world deployments. This choice of accessible, robust technology directly challenges the high-cost, high-complexity paradigm often seen in research from high-income countries.

5.2.3 Development of the System as a Solution

The developed system presents a direct solution to the dual problems of energy shortage and public safety in Zambia. By powering flyover streetlights independently of the national grid, it mitigates the impact of load-shedding. The system is less susceptible to the vandalism that plagues solar streetlights because its core value is not in a easily removable battery but in the integrated system itself. This development directly translates the theoretical potential of vehicle-induced wind into a tangible, deployable product that aligns with the socio-economic realities of the region.

5.2.4 Comparison with Other Similar Works

When compared to prior research, this project carves out a distinct niche:

Unlike the simulation-heavy studies critiqued by Alsahli *et al*. (2025) and Łyskawiński *et al*. (2024), this work is grounded in physical prototyping and practical circuit development, bridging the gap between theoretical models and field-ready implementation.

While Afify *et al*. (2025) [14] focused on a revolutionary blade modification to boost efficiency, this project prioritized system-level integration and techno-economic accessibility. Our work demonstrates that even with a conventional blade design, a functional and valuable system can be built, though their flapping-gate innovation presents a compelling avenue for future efficiency gains.

Compared to the large-scale or grid-connected ambitions of many studies, this project's scope is intentionally targeted and decentralized. It shares the application-focused mindset of Badran *et al*. but addresses their identified scaling problem by designing a complete, miniaturized system from the outset for a specific, low-power load.The explicit design for the Zambian context fills the pronounced geographical bias in the literature, moving beyond the infrastructure and economic assumptions typical of research from high-income countries.

5.2.5 Possible Applications

1. The primary application is the autonomous powering of LED streetlights on flyover bridges and highways. Beyond this, the system can be adapted for:
2. Powering traffic warning signs and signals.
3. Providing auxiliary power for surveillance cameras on transport infrastructure.
4. Serving as an educational model for renewable energy technology in local institutions.

5.3 Summary

In summary, this project has successfully designed,

developed, and validated a prototype mini Savonius turbine system that is technically viable, economically sensible, and contextually appropriate for Zambia. It proves that vehicle-induced wind energy can be a reliable source for critical public infrastructure lighting, offering a sustainable alternative to grid dependence and vandalism-prone solar systems.

5.4 Conclusion

The research conclusively demonstrates that the strategic integration of simple, appropriate technology can harness the untapped wind energy from vehicular movement on flyovers. The developed system effectively addresses the core problem statement by providing a pathway towards illuminated, safe flyover bridges independent of the inconsistent main grid. This work contributes a practical framework for adopting decentralized renewable energy solutions in developing countries, turning a ubiquitous by-product of modern transportation into a source of community resilience and safety.

5.5 Future Works

5.5.1 Advanced Blade Geometry:

Implementing and testing a helical shape for the Savonius turbine to achieve smoother torque and higher efficiency, as empirically validated by Łyskawiński *et al*. (2024).

5.5.2 Enhanced Power Transmission:

Investigating an improved gear system with a higher ratio (e.g., 10:1) to further increase generator input speed and power output, especially at very low wind speeds.

5.5.3 Generator Optimization:

Comparing the performance of a simple, low-cost DC generator against a high-efficiency advanced generator (such as a Permanent Magnet Synchronous Generator) to find the optimal balance between cost, complexity, and power conversion efficiency for this specific application.

5.5.4 Material Science:

Exploring alternative, low-cost, and upcycled materials that offer a better strength-to-weight ratio than PVC for improved longevity and performance.

5.5.5 Long-Term Field Studies:

Deploying multiple units on a chosen flyover for an extended period to gather robust data on maintenance needs, durability, and real-world energy yield across different seasons.

6. Acknowledgment

First and foremost, I give all praise and thanks to Almighty God for the precious gift of life, His unwavering strength, and His countless blessings throughout this journey. Without His grace, this achievement would not have been possible.

I wish to express my profound gratitude to my family and friends for their steadfast love, prayers, and endless encouragement. Your belief in me has been my greatest source of motivation.

My sincere and deepest appreciation goes to my supervisor, Mr. Shabiyemba Mununga, for his invaluable guidance, patience, and expert advice throughout the development of this project. His insights were instrumental in shaping this work.

I am deeply thankful to my friend, Kaunda Mubanga, for his tireless efforts and expertise in helping to design a functional circuit using Proteus. His dedication was crucial to the success of the electronic design phase.

I extend my special thanks to Uncle Nick, for his generous guidance and for teaching me the practical skills of soldering and connecting the physical circuit components. His mentorship bridged the gap between theory and practice.

My genuine gratitude also goes to my friend, Owen Sikochi, for his immense and tireless assistance in the assembly and setup of the turbine. His hard work and supportive partnership were vital during the most challenging stages of the physical construction.

Finally, to all others who contributed in one way or another, I thank you.

7. References

1. Global Wind Atlas. Wind Speeds in Zambia, 2025.
2. Energy Regulation Board. Electricity Supply Industry Report, 2022.
3. Global Wind Energy Council. Wind Energy Developments in Africa, 2025.
4. International Energy Agency. Renewables: Wind Energy Systems, 2025.
5. Wood Mackenzie. Wind Power Outlook, 2025.
6. Ministry of Energy. Draft Report: Strategic Environmental Assessment of the Energy Sector in Zambia, November 2023.
7. Ahmed MR, Islam MQ, Rahman MA. Designing and Manufacturing of Miniature Savonius Wind Turbine, 2016.
8. Han J, Du Z, Pan J, Hu H. Vehicle-Induced Wind Energy Harvesting, 2019.
9. Ehab D. Design Considerations of Highway Wind Turbines and their Integration with Infrastructure, 2018.
10. Duapper F. Feasibility Study on Vertical Axis Wind Turbines, 2020.
11. Rana S, Roy B, Saha BB, Ghosh S. Energy Harvesting from Highway Traffic Vehicles Movement via VAWT. Proceedings of the 8th International Exchange and Innovation Conference on Engineering & Sciences (IEICES). Kyushu University, 2022, 122-127.
12. Roshan A, Goudarzi A. Development of Micro Wind Energy Systems for Transportation Infrastructure, 2022.
13. Passila N. Wind Energy Potential in Urban Areas. Bachelor's Thesis. Metropolia University of Applied Sciences, 2020.
14. Afify R, Saber E, Awad H. Investigation of an innovative Savonius turbine in practice. Scientific Reports. 2025; 15(6937).
15. Johnson KE, Pao LY, Balas MJ, Finger LJ. Control of variable-speed wind turbines: Standard and adaptive techniques for maximizing energy capture. Control Systems, IEEE. 2006; 26(3):70-81.